이학박사학위논문

Tau에 의한 퇴행성뇌질환 모델로서 caspase 절단 형태의 tau를 과발현하는 쥐 분석과 Tau 질환을 조절하는 새로운 유전자 *POLDIP2*의 기능 연구

Study on the characterization of caspase-cleaved tau transgenic mice and genetic modifier *POLDIP2* in tauopathy

2015년 6월

서울대학교 대학원

생명과학부

김 영 두

Tau에 의한 퇴행성뇌질환 모델로서의 caspase 절단 형태의 tau를 과발현하는 쥐 분석과 Tau 질환을 조절하는 새로운 유전자 *POLDIP2*의 기능 연구

Study on the characterization of caspase-cleaved tau transgenic mice and genetic modifier *POLDIP2* in tauopathy

지도교수 정 용 근

이 논문을 이학박사 학위논문으로 제출함

2015년 6월

서울대학교 대학원

생명과학부

김 영 두

김영두의 이학박사 학위논문을 인준함

2013년 6월

위 원 장 _____(인)

부 위 원 장 _____(인)

위 원 _____(인)

위 원 _____(인)

위 원 _____(인)

Study on the characterization of caspase-cleaved tau transgenic mice and genetic modifier *POLDIP2* in tauopathy

A dissertation submitted in partial
Fulfillment of the requirement
for the degree of

DOCTOR OF PHILOSOPHY

to the Faculty of
School of Biological Sciences
at
Seoul National University
by

YoungDoo Kim

Date Approved:
June, 2015

_____

_____

_____

_____

_____

ABSTRACT

Study on the characterization of caspase-cleaved tau transgenic mice and genetic modifier *POLDIP2* in tauopathy

YoungDoo Kim
School of Biological Sciences
The Graduate School
Seoul National University

In Alzheimer's disease (AD) and other tauopathy, Tau proteins form intracellular aggregates and Tau filaments. These tau oligomers are known as one of major cause of neurotoxicity in tauopathy. However, the mechanisms that regulate Tau aggregation are not fully understood. In this study, I approached animal model to better understand the mechanism by generating tau transgenic mouse model showing tau oligomers and by isolating tau aggregation regulator.

In the AD brain, activated caspases cleave tau at the 421th Asp, generating a caspase-cleaved form of tau, TauC3. Although TauC3 is known to assemble

rapidly into filaments *in vitro*, a role of TauC3 *in vivo* remains unclear. Here, I generated a transgenic mouse expressing human TauC3 using a neuron-specific promoter. In this mouse, I found that human TauC3 was expressed in the hippocampus and cortex. Interestingly, TauC3 mice showed drastic learning and spatial memory deficits and reduced synaptic density at a young age (1.3–3 months). Notably, tau oligomers as well as tau aggregates were found in TauC3 mice showing memory deficits. Further, *i.p.* or *i.c.v*. injection with methylene blue or Congo red, inhibitors of tau aggregation *in vitro,* and *i.p.* injection with rapamycin significantly reduced the amounts of tau oligomers in the hippocampus, rescued spine density, and attenuated memory impairment in TauC3 mice. Together, these results suggest that TauC3 facilitates early memory impairment in transgenic mice accompanied with tau oligomer formation, providing insight into the role of TauC3 in the AD pathogenesis associated with tau oligomers.

Also, in this study, we show that *POLDIP2* is a novel regulator of Tau aggregation. From a cell-based screening using cDNA expression library, we isolated POLDIP2 which increased Tau aggregation. Expression of POLDIP2 was increased in neuronal cells by the multiple stresses, including Aβ, TNF-α and H_2O_2. Accordingly, ectopic expression of POLDIP2 enhanced the formation of Tau aggregates without affecting Tau phosphorylation, while

down-regulation of POLDIP2 alleviated ROS-induced Tau aggregation. Interestingly, we found that POLDIP2 overexpression induced impairments of autophagy activity and partially proteasome activity and this activities were retained in DUF525 domain of POLDIP2. In a drosophila model of human tauopathy, knockdown of the drosophila *POLDIP2* homolog, CG12162, attenuated rough eye phenotype induced by Tau overexpression. Further, the lifespan of neural-Tau^{R406W} transgenic files were recovered by CG12162 knockdown. Together, these observations indicate that POLDIP2 plays a crucial role in Tau aggregation via the impairment of autophagy activity, providing insight into mechanism that regulates Tau aggregation in Tau pathology.

Keywords: Caspase-cleaved tau, tauopathy, Alzheimer's disease, tau oligomers, POLDIP2, proteasome, autophagy, lifespan

***Student Number*:** 2007-30769

CONTENTS

LIST OF FIGURES AND TABLES

ABBREVIATIONS

AD	Alzheimer’s disease
DMEM	Dulbecco's Modified Eagle's Medium
DMSO	Dimethyl sulfoxide
EDTA	Ethylenediaminetetraacetic acid
FBS	Fetal Bovine Serum
GFP	Green Fluorescence Protein
GFP-Tau	Green fluorescent protein-Tau fusion protein
H_2O_2	hydrogen peroxide
kDa	Kilodalton
NEM	*N*-Ethylmaleimide
PBS	Phosphate Buffered Saline
RIPA	Radio-Immunoprecipitation Assay
PMSF	Phenylmethylsulfonyl fluoride
ROS	reactive oxygen speicies
SDS-PAGE	Sodium Dodecyl Sulfate-Poly Acrylamide Gel Electrophoresis
shRNA	short-hairpin RNA

SPF	Specific Pathogen Free
TBST	Tris Buffered Saline with Tween-20
Tris	Tris (hydroxymethyl) aminomethane
UPS	ubiquitin proteasome system

CHAPTER 1

Caspase-cleaved tau exhibits rapid memory impairment associated with tau oligomers in a transgenic mouse model

Abstract

In neurodegenerative diseases like Alzheimer's disease (AD), tau is hyperphosphorylated and forms neurofibrillary tangles in affected neurons. In the AD brain, activated caspases cleave tau at the 421th Asp, generating a caspase-cleaved form of tau, TauC3. However, its role in AD pathogenesis remains unclear. To evaluate *in vivo* activity of TauC3, I generated a transgenic mouse expressing human TauC3 using a neuron-specific promoter. In this mouse, I found that human TauC3 is expressed in the hippocampus, cortex, and cerebellum with comparable level to mouse tau. TauC3 mice showed drastic learning and spatial memory deficits and reduced synaptic density at a young age (2–3 months). Compared to control mice, tau protein in TauC3 mice was highly phosphorylated at many epitopes, including PHF-1 and AT100. Notably, both detergent-soluble tau oligomers and detergent-insoluble tau aggregates were found in TauC3 mice showing memory deficits and its level increased during aging. Intraperitoneal injection of TauC3 mice with methylene blue, an inhibitor of tau aggregation *in vitro*, significantly reduced the amounts of tau oligomers and aggregates in the hippocampus and attenuated memory impairment. Together, these results suggest that TauC3 facilitates the formation of tau oligomers and aggregates *in vivo* and induces

memory impairment in transgenic mice, providing insight into the role of TauC3 in the AD pathogenesis associated with tau aggregates.

Introduction

Tau is a neuronal microtubule-associated protein that binds to and stabilizes microtubules in axons (Schweers et al., 1994). In AD and other tauopathies, Tau is hyperphosphorylated and forms insoluble aggregates called neurofibrillary tangles (NFTs) in neurons (Lee et al., 2001). While NFTs are considered as a hallmark of AD (Braak and Braak, 1991), it is unlikely that NFTs are the major toxic Tau species (Santacruz et al., 2005). Recently, Tau oligomers and aggregates were detected in the brain of AD model mice and proposed to play an important role in AD pathogenesis (Berger et al., 2007). It appears that intermediate forms of Tau, which are highly phosphorylated, may form before the NFT development and mediate neuronal dysfunction (Lasagna-Reeves et al., 2011).

Many Tau mouse models have been established for studying tauopathy. Because normal Tau protein is too soluble to form Tau aggregates, however, transgenic (TG) mice expressing wild-type human Tau or Tau kinase do not show either NFTs or memory loss in most cases (Duff et al., 2000; Gotz et al., 1995; Lucas et al., 2001). Tau TG model expressing a missense mutation shown in a frontal temporal dementia with Parkinsonism linked to

chromosome 17 (FTDP-17) patient reveals neuronal loss with hyperphosphorylated Tau and an NFT-like Tau aggregate, but no associated memory deficits (Lewis et al., 2000). rTG4510, a TRE-inducible mouse model overexpressing P301L Tau mutant, shows memory loss with hyperphosphorylated Tau at early age and NFT formation at middle age (Santacruz et al., 2005). However, overexpression of P301L Tau mutant is too high in this case. Also, in AD and other tauopathy without FTDP-17, P301L mutation is not found in *Tau* gene despite there being an aggregation of Tau in neurons (Wolfe, 2009). Currently, existing mouse models are not sufficient to describe the spectrum of tauopathy, especially Tau oligomers and aggregates-associated memory impairment.

Because of Aβ and stress, caspases are activated in the AD brain and cleave multiple proteins, including Tau (Rohn et al., 2002). TauC3 has been shown to form Tau oligomers and aggregates faster than wild-type Tau *in vitro* (Gamblin et al., 2003), and localized within Tau aggregates in P301S and rTG4510 mice (Delobel et al., 2008; Zhang et al., 2009). In the brain of rTG4510 mice, caspase activation leads to the formation of tangles in cells just a day after and TauC3 is found in tangles (de Calignon et al., 2010). In addition, TauC3 is typically found in the brain of patients at the mild cognitive impairment stage of AD (Gamblin et al., 2003; Rissman et al., 2004) and those

with other tauopathies, including Pick's disease (Mondragon-Rodriguez et al., 2008), corticobasal degeneration (Newman et al., 2005), progressive supranuclear palsy (Guillozet-Bongaarts et al., 2005), and traumatic brain injury (Gabbita et al., 2005). These data indicate that TauC3 is associated with Tau aggregates. However, the role of TauC3 in AD pathogenesis, whether TauC3 is byproduct or cause of the pathology, remains unknown.

In this study, I show that transgenic expression of TauC3 in the mouse brain induces memory impairment at a young age, which is accompanied by the appearance of Tau oligomers and aggregates. Aggregation blockers, such as methylene blue and Congo red, inhibit Tau aggregation and prevent memory impairment in the TauC3 mice. Thus, TauC3 oligomers and aggregates are able to participate in AD pathogenesis.

Materials and methods

Generation of TauC3 mice

The human *tau* expression construct was injected into embryos and positive F_0 mice were identified by PCR analysis using a synthetic oligonucleotide (forward; 5′-GGA TGG CTG AGC CCC GCC CGG AGT TCG-3′) corresponding to the *BAI1-AP4* promoter and an oligonucleotide (reverse; 5′-GGG CTG CTC GCG GTG TGG CGA TCT TC-3′) of *tau* cDNA (Macrogen Inc., Korea). TauC3 mouse was identified and mated to FVB WT mice to generate a pure FVB genetic background for the F_2 generation, and F_3 offspring was then backcrossed to BALB/C mice under a 12: 12 h of light: dark cycle with access to food and water *ad libitum*.

Western blot analysis

The cortex, hippocampus, cerebellum, striatum, and other brain regions were prepared from TauC3 mice and age-matched littermates (6 to 10 mice per age). Subsectioned brain tissues were grinding with a mortar and pestle in liquid nitrogen and powdered tissues stored at - 80°C until use. The powdered tissues were homogenized in 3 different extraction buffers for the purpose.

First, TBS extraction buffer [20 mM Tris-Cl (pH 7.4), 1 mM phenylmethylsulfonyl fluoride (PMSF), 1 mM Na_3VO_4, and 20 mM NaF with 0.5 % NP-40] to detect tau phosphorylation. Second, oligomer extraction buffer [20 mM Tris-Cl (pH 7.4), 0.8 M NaCl, 10 % sucrose, 1 mM ethylene glycol tetraacetic acid (EGTA), 1 mM PMSF, 1 mM Na_3VO_4, 20 mM NaF, and 0.5 % NP-40] containing 2 mM NEM. Third, RAB buffer [0.1 M 2-(N-morpholino) ethanesulfonic acid (MES) pH 7.0, 1 mM EGTA, 0.5 mM MgSO4, 0.75 M NaCl, 1 mM PMSF, 1 mM Na_3VO_4, and 20 mM NaF] and RIPA buffer, (50 mM Tris-Cl pH 8.0, 150 mM NaCl, 0.5 % NP-40, 5 mM EDTA, 0.5 % sodium deoxycholate, and 0.1 % SDS) were prepared to solubilize RIPA-insoluble Tau. Samples were then solubilized in SDS sample buffer with or without β-mercaptoethanol to examine different Tau species with Western blotting.

Antibodies

TG5 (total Tau: detects epitope a.a.220-240, 1:1,000), PHF-1 [p-Tau: Ser396/404, later-stage NFTs (Uboga NV and Price JL., 2000), 1:3,000], CP13 (p-Tau: Ser202, 1:1,000), and MC1 [a conformational abnormality of Tau (Jicha et al., 1997), 1:500 antibody] were kindly gifted from Dr. P. Davies (Albert Einstein College of Medicine, NY, USA). 12E8 (p-Tau:

Ser262/Ser356, 1:3,000) was kindly gifted from Dr. P. Seubert (Elan Pharmaceuticals, MA, USA). AT8 (p-Tau: Ser202/205, 1:3,000), AT100 [p-Tau: Ser212/214, Alzheimer-associated abnormal Tau (Weaver et al., 2000), 1:5,000], pT231 (p-Tau: Ser231, 1:3,000), and HT7 (human Tau-specific: 159 and 163, 1:5,000) antibodies were purchased from Thermo scientific (IL, USA). TauC3 (1:2,500) antibody was from Invitrogen (CA, USA) and Tau3 antibody (1:100) was generated against a peptide containing Asp421. ATG5 (1:2,000), LC3 (1:3,000), and p62 (1:1,000) antibodies were from Novus biologicals (CO, USA). P-S6 (1:1,000) PSD95 (1:1,500), NR1 (1:1,000), NR2A (1:1,000) and NR2B (1:1,000) antibodies were from Cell signaling (MA, USA). Tubulin (1:10,000) and β-actin (1:10,000) antibodies were from Santa Cruz biotechnologies (DL. USA). Secondary mouse (1:10,000) and rabbit (1:10,000) antibodies conjugated to peroxidase were purchased from Jackson Immunoresearch (PA, USA).

Cell culture, DNA construction, and DNA transfection

SH-SY5Y (human neuroblastoma) cells and primary hippocampal neurons were prepared as described previously (Park et al., 2012). Briefly, SH-SY5Y cells were cultured in DMEM (Hyclone) supplemented with 10 % (v/v) fetal bovine serum (Hyclone). Primary hippocampal neurons were cultured from

postnatal day 1 and incubated for 13 days in neurobasal media containing B27 (Invitrogen). SH-SY5Y cells were transfected using the Polyfect reagent (Quiagen), whereas primary neurons were transfected using the Lipofectamine 2000 reagent (Invitrogen) according to the manufacturer's instructions. Tau-GFP and TauC3-GFP constructs were described previously (Chung et al., 2001).

Dendritic spine density analysis

Dendritic spine density analysis was described previously (Kam et al., 2013). In brief, cultured hippocampal primary neurons were transfected at 13 days *in vitro* (DIV) with EGFP-fusion construct for 24 h. Images of GFP-expressing cells were acquired by confocal microscopy (Carl Zeiss) and the numbers of spines on the axon (100 μm in length) of randomly chosen neurons were counted on the images ($n = 6 \sim 10$).

***In vitro* Tau fibrillation and thioflavin T fluorescence assay**

Tau construct was previously described (Chung et al., 2001). Human full-length *tau* (0N4R) was subcloned into pET28a containing histidine (His^{6x}) (Invitrogen) to generate His-fusion protein ($pHis^{6x}$-Tau) and Tau protein was purified from bacteria (BL21-DE3) after transformation with $pHis^{6x}$-Tau.

Total 10 μM Tau protein was incubated with 50 mM NH_4Ac buffer containing 20 μM heparin and 2 mM dithiothreitol at 37°C. The reaction products were then incubated with 25 μM thioflavin T (Sigma) (final concentration was 5 μM) and fluorescence was measured with a LS-50 fluorimeter (Perkin-Elmer) using an excitation filter of 450 nm and an emission filter of 484 nm.

Filter trap assay

The filter trap assay of Tau protein was performed as previously described (Park et al., 2012). Tissue extracts were prepared in TBS extraction buffer by sonication. After centrifugation at 15,000x *g* for 30 min at 4°C, the supernatants were incubated with 0.1 % SDS for 30 min. After incubation, supernatants were filtered through nitrocellulose membrane (0.2 μm) (Pall industries) by using a 96-well vacuum dot blot apparatus (Bio-Rad laboratories). The membrane was washed twice with TBST, blocked with TBST containing 5 % non-fat milk for 1 h, and analyzed by Western blotting.

Histology and immunohistochemistry

Mice were transcardially perfused with ice-cold PBS before dissection of the tissue post fixation. Histological and immunohistochemical analysis were performed on 25-μm thick coronally cut cryosectioned free-floating sections.

Immunohistochemistry was done using standard immunoperoxidase procedures with Elite ABC kits (Vector Laboratories) and developed with 3,3-diaminobenzidine. The following monoclonal antibodies were used to stain the free-floating brain sections: HT7 (1:100), TauC3 (1:50), PHF-1 (1:100), AT100 (1:1000), T22 (1:100), MC-1 (1:10), synaptophysin (1:100, Santa Cruz Biotechnology), and GFAP (1:1000, Santa Cruz Biotechnology).

Behavior tests

Behavior test was performed as previously described (Kam et al., 2013). TauC3 mice and age-matched wild-type controls (were tested for 3 different types of memory and 1 motor function: Y-maze test has been longitudinally performed from 1.3 to 6 months of age for 3 week interval (between 1.3 and 2 month) and for 1 month interval (from 2 to 6 months) for spatial memory. Noble object recognition and passive-avoidance tests were done from 1.3 to 6 months of age and wire-hang test was performed to evaluate motor function and deficit. Number of animals are different and both male and females are used. (n = 11–19 mice per group. Figure 2; WT, 10 males and 8 females; TauC3, 10 males and 9 females. Figure 6; WT PBS, 6 males and 5 females; WT methylene blue, 5 males and 6 females; TauC3 PBS, 10 males and 8 females; TauC3 methylene blue, 9 males and 9 females; TauC3 Congo Red,

6 males and 5 females. Figure 8; WT PBS, 6 males and 6 females; WT rapamycin, 7 males and 6 females; TauC3 PBS, 10 males and 9 females; TauC3 rapamycin, 8 males and 9 females.)

Y-maze: This test is well known to evaluate spatial memory of mice. A triangular Y-maze was made from black plastic with arm size of 32.5 cm x 15 cm (length x height). For the test, mice were placed in the end of one arm and allowed to move freely through the maze for 7 min. An entry was defined as placing all four paws into the arm. The percentage of spontaneous alterations was calculated as the ratio of the number of successful alterations to the number of total alterations. After each trial, the maze was cleaned with 70 % ethanol.

Y-maze spontaneous alternation test: This is a behavioral test for measuring hyperactivity and general locomotor activity. Method is similar with Y-maze test; mice were placed in the end of one arm and allowed to move freely through the maze for 7 min, but instead ratio of the number of successful alterations, total number of arm entry were counted and identified as hyperactivity and locomotor activity.

Novel object recognition test: This test is to evaluate cognition, particularly recognition memory of mice. Mice were first habituated in a white plastic chamber (22 cm wide x 27 cm long x 30 cm high) for 7 min with

24 h intervals. After 2 days (training trial), the mice were presented with two objects and allowed to explore freely for 7 min. In the testing trial, performed 24 h later, one of the familiar objects was changed for a novel object and mice were scored for recognition during 7 min. The object recognition was defined as spending time with orienting toward the object in a distance of 1 cm or less, sniffing the object or touching with the nose. Between each trial, the arena and objects were wiped down with 70 % ethanol.

Passive avoidance: The passive avoidance apparatus consists of a light (white) and dark (black) compartments (20 x 20 x 20 cm each) separated by a guillotine door. The floor of the dark compartment was made of stainless-steel grids. During habituation, mice were allowed to freely explore the box for 5 min with the door open and then returned to their home cage. For conditioning, after 24 h, mice were placed into the light compartment and the sliding door was closed when both hind limbs of mice were entered into the dark box and an electric foot shock (0.2 mA, 1 sec) was then delivered by the floor grids. Ten seconds later, the mice were returned to their home cage. Tests were carried out 24 h after the conditioning and the latency time for mice to enter the dark compartment was measured with a 7 min cut-off.

Wire-hang test: The test began with the animal hanging from an elevated wire cage top. The animal was placed on the cage top, which was then

inverted and suspended above the home cage 60 cm high. When mice fell down, latency to fall was recorded.

Intracerebroventricular injection of Aβ oligomers

Generation of Aβ1-42 (Aβ) oligomers and intracerebroventricular injection of Aβ oligomers (H-2972; Bachem) into the mice are described previously (5).

Results

Generation of a neuron-specific TauC3 transgenic mouse.

To examine the role of TauC3 in memory impairment, I generated TauC3 mice expressing a short isoform of 4 repeat (0N4R) human Tau lacking the C-terminus 20 amino acids. Caspase cleavage product of 0N4R Tau (0N4R $tau_{1\text{-}363}$) corresponding to 2N4R Tau (2N4R $tau_{1\text{-}421}$) was expressed under the control of a brain-specific angiogenesis inhibitor 1-associated protein 4 (BAI1-AP4) promoter (Kim et al., 2004). The BAI1-AP4 promoter in the BAI1-AP4/β-galactosidase transgenic mice drives neuron-specific expression of β-galactosidase in the sub-regions of the brain, mainly in the cortex and hippocampus. Accordingly, the results from Western blot analysis using human Tau-specific HT7 antibody revealed that TauC3 with a molecular weight of 50 kDa was detected in a number of brain areas, including the cortex, hippocampus, striatum, and cerebellum of TauC3 mice (Fig. 1-2A). Using TauC3 antibody, a caspase 3-cleaved Tau-specific antibody (Gamblin et al., 2003), I also found the same size of Tau protein only in TauC3 mice but not in wild-type mice (Fig. 1-2A). On the other hand, human TauC3 was not detected in the peripheral tissues of TauC3 mice (Fig.

1-1).

When I examined both mouse and human Tau proteins by Western blot analysis using TG5 antibody, the amount of total Tau protein was about 16% (cerebellum) to 54% (hippocampus) higher in TauC3 mice than in wild-type littermates (Fig. 1-2B). Examination of tissue- and cell type-specific expression of TauC3 using immunohistochemical analysis revealed that HT7-positive human TauC3 was largely expressed in the cortex and hippocampus of TauC3 mice (Fig. 1-1B). In addition, HT7 and TauC3 antibodies detected human TauC3 in the layer I to II of cerebral cortex, and in the CA3 pyramidal cell layer and mossy fiber layer of the hippocampus in TauC3 mice (Fig. 1-3), important regions for spatial memory and long-term memory consolidation.

Impaired memory function and reduced synaptic density in TauC3 mice at an early age.

I then measured memory function of TauC3 mice. The results from Y-maze test revealed that spatial working memory was drastically impaired at 2 months and completely lost at 4 months in TauC3 mice (0.73 to 0.55) (Fig. 1-4A). In the novel object recognition test, control littermates spent more time

exploring the novel object than the object previously explored 1 day before (Fig. 1-4B). In contrast, TauC3 mice showed impaired preference to the new object at when they were 2 months old, and this impairment continued to worsen until 5 months of age (67 % to 56 %). In both tests, memory function started to be impaired as early as at 1.3 months in TauC3 mice (Fig. 1-4A and B). I also examined TauC3 mice on passive avoidance memory test. During training, learning and memory represented by escape latency was slowed at around 2 months in TauC3 mice. Specifically, TauC3 mice showed a deficit in recalling an electric shock given a day before, in which escape latency decreased from 363 sec to 78 sec during 1.3 to 5 months of age (Fig. 1-4C). Together, these results suggest that TauC3 mice show learning and memory impairments as early as 2 months of age. While TauC3 was detected in the cerebellum of the transgenic mice, wire-hang test revealed little difference between TauC3 and age-matched wild-type mice in motor weakness or muscle atrophy (Fig. 1-5A) and Y-maze spontaneous alternation test showed no difference in hyperactivity (Fig. 1-5B).

Because synaptic integrity is closely associated with memory function in AD, I compared synaptic density in aging TauC3 and wild-type mice. An immunohistochemical analysis revealed that the synaptophysin, a synaptic vesicle protein reflective of synaptic density (Masliah et al., 1989), began to

decrease in the hippocampal CA3 mossy fiber layer in 1.3 month-old TauC3 mice and were more reduced at 3 months compared to control littermates (Fig. 1-6A and B). Investigation of the synaptic proteins with Western blotting revealed that the levels of postsynaptic density-95 (PSD95), N-methyl-D-aspartic receptors 1 (NR1), and 2B (NR2B) significantly decreased in the hippocampus of 3 and 6 month-old TauC3 mice (Fig. 1-6C and D). Together with the memory impairments, age-dependent reduction of synaptic density in TauC3 mice may cause the observed memory impairment through synaptic dysfunction.

On the other hand, examination of cell death showed a few of TUNEL-positive signals (1.25 ~ 3.25/mm^2) in the hippocampus and cortex of 6 month-old TauC3 mice and its increase in 12 month of age (Fig. 1-7) but no significant reduction in total cell numbers of the affected tissues (Fig. 1-8). There was no significant difference in life span until 22 months between wild-type and TauC3 mice (Fig. 1-9).

Appearance of Tau oligomers in TauC3 mice showing memory deficit.

To gain insight into the mechanism by which TauC3 produces memory deficits, I analyzed Tau phosphorylation. From Western blot analysis using

various phospho-Tau-specific antibodies, I found that Tau phosphorylation at PHF-1 (Ser 396/404) epitope was already detected in the hippocampus of 1.3 month-old TauC3 mice and increased further until 3 months (Fig. 1-10). Additionally, conformation change of Tau protein detected by an MC-1 antibody was apparent in the brains of 1.3 and 2 month-old TauC3 mice (Fig. 1-10). These data show that Tau hyperphosphorylation occurs in TauC3 mice showing memory impairment.

Different Tau species, frequently seen as both detergent-soluble and -insoluble Tau, have also been implicated in AD pathogenesis (Hanger et al., 1991; Kopeikina et al., 2012). Thus, I investigated the presence of detergent-soluble Tau oligomers in TauC3 mice. To identify the Tau oligomers, mouse hippocampal lysates were resolved in the lysis buffer containing N-ethylmaleimide (NEM) which protects native disulfide bonds but prevents non-specific disulfide bond formation after cell lysis (Molinari and Helenius, 1999). Unlike reducing condition, a Western blot analysis under a non-reducing condition lacking β-mercaptoethanol and DTT revealed a high molecular weight (around 170 kDa) of human Tau (HT7) in TauC3 mice but not in wild-type littermates. (Fig. 1-11A). Interestingly, 170 kDa human Tau was first observed in the hippocampus of TauC3 mice at 1.3 month of age and its level increased until 3 months, whereas 50 kDa human Tau was not

detected.

On the contrary, Western blotting using a TG5 antibody under the same condition revealed that the half of the total Tau protein was detected at 50 kDa and the other half at 170 kDa. The majority of Tau signal was detected at 170 kDa in TauC3 mice by PHF-1, MC-1, and Tau oligomer-specific T22 (Lasagna-Reeves et al., 2012) antibodies and these signals further increased with aging (Fig. 1-11B and C). Analysis of other AD model mice, 3X TG mice which express APP^{swe}, PS, and Tau P301L (Oddo et al., 2003), revealed the presence of both 170 kDa and 50 kDa human Tau in 9 month-old mice showing memory impairment but 170 kDa Tau was not in 2 month-old mice with normal memory function (Fig. 1-11D). From an immunohistochemical analysis, I also observed the hyperphosphorylated Tau oligomers in the hippocampus of TauC3 mice; HT7- and T22-positive Tau oligomers were localized in the pyramidal cell layer and PHF-1-positive Tau in the mossy fiber layer of the hippocampal CA3 region (Fig. 1-12). Together, the results indicate that TauC3 in TauC3 mice is present exclusively as oligomers which are highly phosphorylated. Additionally, from immunohistochemical analysis, I found that caspase inhibitor blocked the formation of T22-positive Tau oligomers and the loss of synaptic density in Aβ oligomer-treated primary neurons (Fig. 1-13). Further, Aβ oligomer-injection assays revealed that

caspase inhibitor blocked the generation of TauC3 and T22-positive Tau oligomers in the brain of the mice showing memory deficit (Fig. 1-14), demonstrating the pathophysiologic role of endogenous TauC3 in mice.

Accumulation of detergent-insoluble Tau aggregates in TauC3 mice.

To examine detergent-insoluble Tau aggregates, Tau protein was serially extracted from hippocampal lysates into an aqueous-soluble (RAB), detergent (NP-40)-soluble, and detergent-insoluble but 70 % formic acid (FA)-soluble Tau fractions. A Western blot analysis of the fractions with a TG5 antibody revealed that compared to wild-type mice, the total amount of detergent-insoluble but FA-soluble Tau was detected in the brain of TauC3 mice at 1.3 months and increased in TauC3 mice in an age-dependent manner (Fig. 1-15A and B). Interestingly, HT7-positive human TauC3 and MC-1-positive Tau with conformational change were detected in the detergent-insoluble fraction and their amounts increased during aging of TauC3 mice, although there was some variation between the mice.

Similarly, a filter trap assay followed by a dot blot analysis revealed that sodium dodecyl sulfate (SDS)-resistant insoluble Tau aggregates were detected in 2 and 3 month-old TauC3 mice and increased during aging (Fig.

1-15C and D). These results indicate that NP-40- or SDS-insoluble aggregates of Tau as well as Tau oligomers accumulate in the hippocampus of TauC3 mice showing memory impairment. Moreover, silver staining-positive Tau aggregates were detected at 3 months in the cortex and hippocampus of TauC3 mice and further increased at 6 months (Fig. 1-16A). Electron microscopic analysis following an immunoprecipitation assay also showed Tau aggregates with filamentous structure in 1.3 month-old TauC3 mice and more of them in 6 month-old TauC3 mice (Fig. 1-16B), as Tau oligomers and detergent-insoluble Tau aggregates increased with aging.

Methylene blue improves memory function and synaptic density with reduced Tau oligomers in TauC3 mice.

To investigate the pathologic significance of Tau oligomers and aggregates, I decided to test the effect of methylene blue and Congo red, which are supposed to be β-sheet aggregation blockers, on the pathology in TauC3 mice. Methylene blue is now in phase III clinical trials for drug development in AD (Gravitz, 2011), but the mechanisms by which it alleviates AD pathology are not yet clearly shown. As reported (Pickhardt et al., 2005), our results from an *in vitro* aggregation assay showed that purified Tau proteins, over time,

began to form thioflavin T (ThT)-positive aggregates in the presence of heparin (Fig. 1-17A). Expectedly, the formation of Tau aggregates was hampered by the addition of methylene blue. In SH-SY5Y cells, methylene blue reduced the amount of filter-trapped Tau aggregates (Fig 1-17B). These results indicate that methylene blue blocks the formation of Tau aggregates *in vitro* and in cells. Please note that high dose of methylene blue could reduce the amount of total Tau as well in cells (Fig 1-17B). Congo red is also known to ameliorate the pathogenesis of Huntington's disease and binds to β-sheet aggregates (Sanchez et al., 2003). In our assay, Congo red also inhibited the formation of Tau aggregates (Fig. 1-17B).

Then I addressed the effects of these molecules on the memory in TauC3 mice. After daily *i.p.*-injection of methylene blue for 30 days or biweekly intracerebroventricular (*i.c.v.*)-injection with Congo red (Fig. 1-18A), memory in TauC3 mice was examined. Spatial and recognition memories in TauC3 mice were not impaired by the treatment with methylene blue and less but still significantly by Congo red (Fig. 1-18B). In contrast, daily *i.p.*-injection of Congo red did not affect memory impairment in TauC3 mice (Fig. 1-19). It may be due to the poor ability of Congo red to penetrate the blood-brain barrier (Wood et al., 2007). These results indicate that Tau aggregation blockers like methylene blue and Congo red can effectively rescue memory

impairment in TauC3 mice.

When I analyzed the effect of methylene blue on the formation of Tau oligomers, Western blot analysis revealed that the amount of Tau oligomers (170 kDa) was remarkably reduced in TauC3 mice after exposure to methylene blue (Fig. 1-20). In the same tissue, the amount of total Tau (TG5) was a little reduced by methylene blue, whereas TauC3 (HT7) and PHF-1 Tau were largely affected (Fig. 1-21). An immunohistochemical analysis showed similar patterns; TauC3 and T22-positive Tau oligomers were apparently reduced in TauC3 mice (Fig. 1-22). Interestingly, unlike full-length Tau, overexpression of TauC3 alone or co-expression with full-length Tau apparently reduced spine density in the primary hippocampal neurons (Fig. 1-23A and B). Consistent to the previous reports (Gamblin et al., 2003; Rissman et al., 004), TauC3 stimulated the formation of ThT-positive Tau filaments and aggregates *in vitro* and in cells. Moreover, methylene blue was potent to block the loss of spine density triggered by TauC3 in cultured neurons (Fig. 1-23A and B) and rescued the loss of synaptic proteins, such as PSD95 and NR1, in TauC3 mice (Fig. 1-23C).

Rapamycin attenuates memory deficits in TauC3 mice.

I further examined the effects of rapamycin, a mTOR inhibitor and autophagy inducer that has been tested in Huntington's disease, Parkinson's disease, and AD (Bove et al., 2011; Caccamo et al., 2010; Ravikumar et al., 2004), on clearing the aggregated Tau. One month-old TauC3 mice were daily injected with rapamycin for 30 days and examined for memory impairment. On a Y-maze test at 30 days after drug treatment, rapamycin rescued memory impairment in TauC3 mice (56.5 % to 65.4 %) almost to the control level (68.4 %). Novel object recognition test also illustrated that recognition memory was improved (0.57 to 0.66). On both tests, rapamycin did not significantly affect memory in wild-type mice. (Fig. 1-24)

Rapamycin greatly reduced the levels of phospho-Tau (PHF-1) and AT100-positive soluble Tau in TauC3 mice, while the level of total Tau was not much changed, and reduced the amounts of NP-40-soluble PHF-1 Tau and NP-40-insoluble (70% FA-soluble) Tau aggregates (Fig. 1-25). In the same experiments, I found that the level of LC3-II, an autophagy marker (Kabeya et al., 2000), increased in the brain of TauC3 mice, while p62, an ubiquitin-binding autophagy marker (Pankiv et al., 2007), decreased by rapamycin (Fig. 1-26). As expected, rapamycin seemed to enhance autophagy flux in the brain of TauC3 mice. Western blot analysis under non-reducing condition revealed that rapamycin reduced the amount of Tau oligomers (170 kDa) in TauC3

mice but less than methylene blue (Fig. 1-27). It appears that rapamycin functions to improve memory in TauC3 mice with enhanced clearance of Tau oligomers and aggregates, probably due to its stimulatory effects on autophagy.

Together with the memory rescue effects by methylene blue and rapamycin, both of which were shown to affect the amounts of Tau oligomers and aggregates, respectively, TauC3 mouse may be a useful AD model to elucidate Tau oligomer-associated pathogenesis of tauopathy and to evaluate therapeutic drug options.

Figure 1-1 **TauC3 mice display neuronal-specific expression of human tau.** (A) Neuronal expression of TauC3. The cortex, hippocampus, spinal cord, heart, lung, liver, kidney, and spleen were isolated from 1.3 month-old wild-type (WT) and TauC3 mice and tissue extracts were analyzed by Western blotting using human Tau-specific HT7 antibody. n.s.; non-specific signal. (B) Immunohistochemical analysis showing the regional expression of TauC3 in the cortex (a) and hippocampus (b) of 1.3 month-old TauC3 transgenic mice. Scale bars, black: 500 μm, red: 200 μm.

A

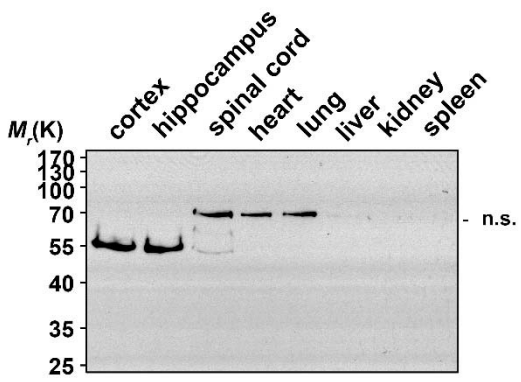
cortex
hippocampus
spinal cord
heart
lung
liver
kidney
spleen
M_r(K)
170
130
100
70
55
40
35
25
n.s.

B

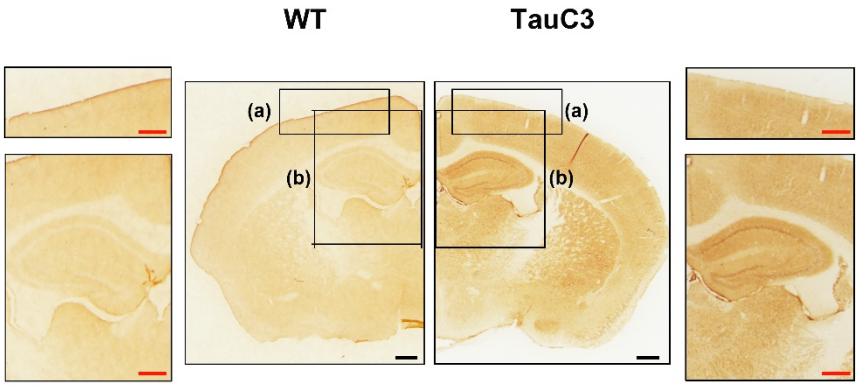
WT
TauC3
(a)
(b)
(a)
(b)

Figure 1-2 **Expression of human caspase-cleaved Tau in the brain region of cortex, hippocampus, cerebellum and striatum of transgenic mice.** (**A**) Transgenic expression of human TauC3 in the mouse brain. Tissue extracts from 1.3-month-old wild-type (WT) and TauC3 mice were analyzed by Western blotting using human Tau (HT7), TauC3-specific (TauC3), and total Tau (TG5) antibodies. (**B**) Densitometric analysis of total human TauC3 and mouse Tau on the blot in (A). Data are means ± SEM (n = 3).

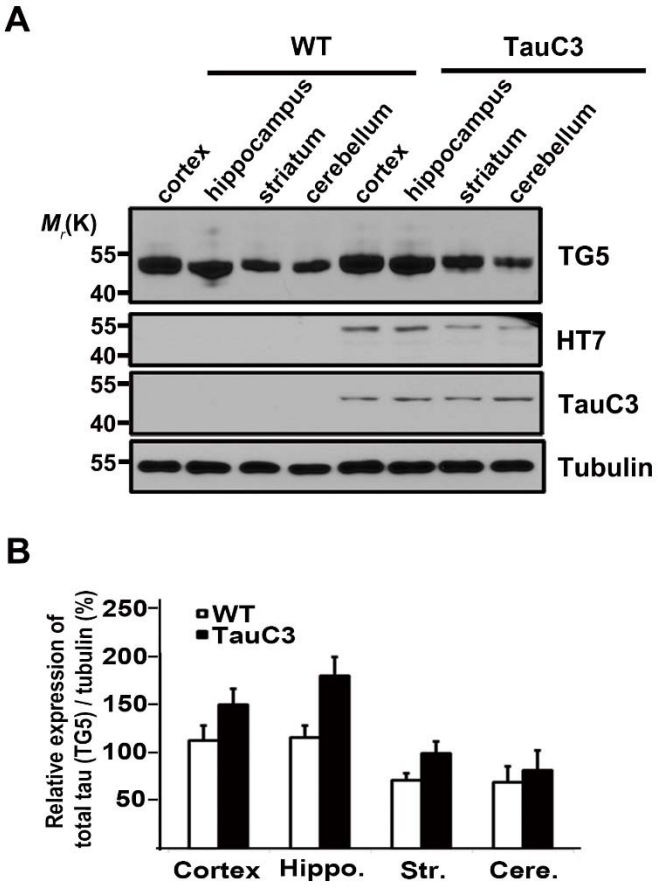
A
WT
TauC3
cortex
hippocampus
striatum
cerebellum
cortex
hippocampus
striatum
cerebellum
M_r(K)
55
40
TG5
HT7
TauC3
Tubulin
B
Relative expression of total tau (TG5) / tubulin (%)
250
200
150
100
50
WT
TauC3
Cortex
Hippo.
Str.
Cere.

Figure 1-3. Human TauC3 is expressed in cortex and hippocampus of TauC3 mice.

Immunohistochemical analysis of Tau in the brain of TauC3 mice. The cortex and hippocampus of 1.3 month-old WT and TauC3 mice were immunostained with HT7 and TauC3 antibodies. Scale bars, black: 400 μm, red: 100 μm.

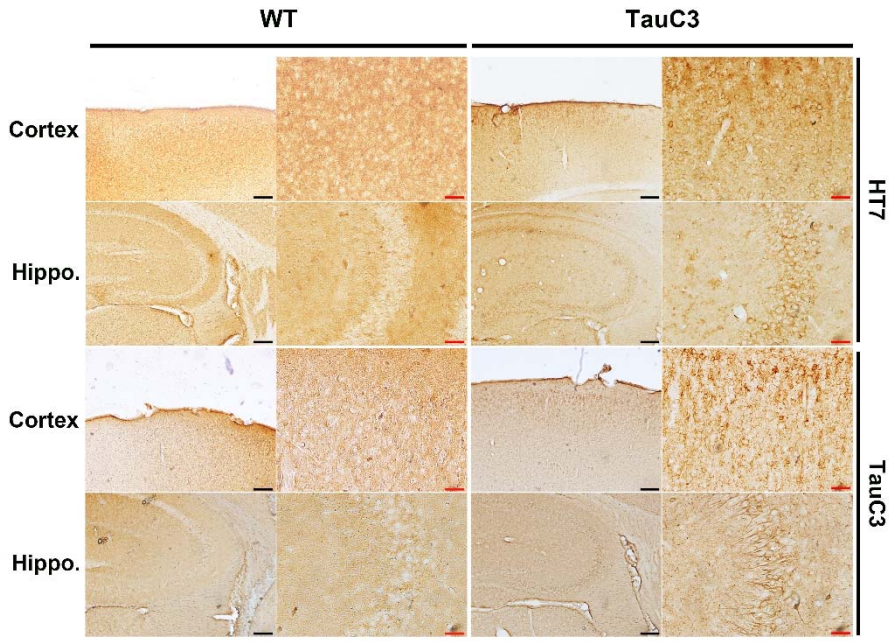
WT
TauC3
Cortex
Hippo.
Cortex
Hippo.
HT7
TauC3

Figure 1-4. Rapid memory impairment in TauC3 mice.

(A - C) Memory deficits in TauC3 mice**.** Wild-type **(**WT) and TauC3 mice were examined for their spatial memory with a Y-maze test (A), recognition memory with a novel object recognition test (B), and cognitive learning memory with a passive avoidance test (C). Data are means ± SEM (n = 19).

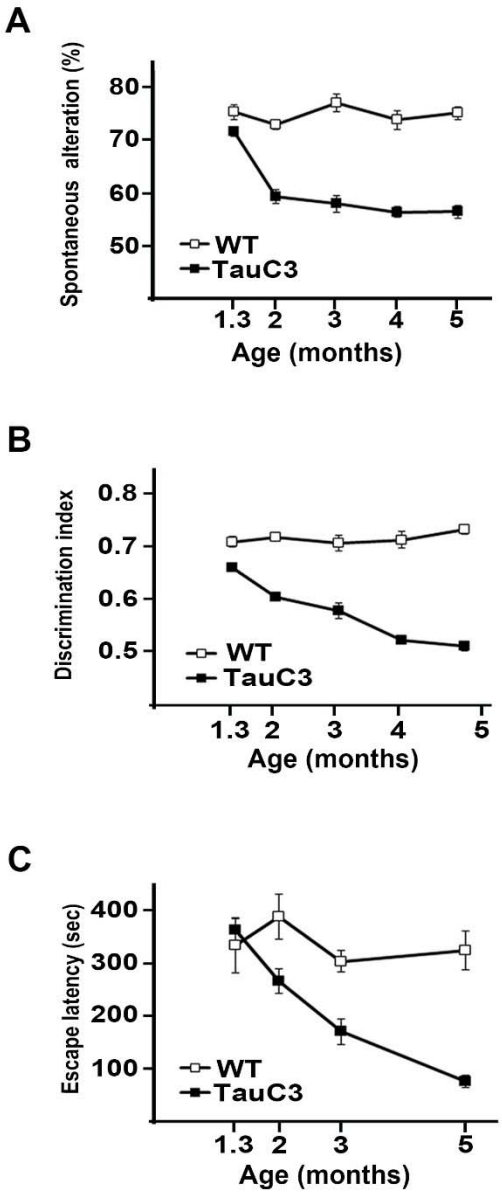
A
Spontaneous alteration (%)
80
70
60
50
WT
TauC3
1.3
2
3
4
5
Age (months)
B
Discrimination index
0.8
0.7
0.6
0.5
WT
TauC3
1.3
2
3
4
5
Age (months)
C
Escape latency (sec)
400
300
200
100
WT
TauC3
1.3
2
3
5
Age (months)

Figure 1-5. TauC3 mice does not show severe behavior abnormality.

(A) TauC3 mice show similar motor function as wild-type mice do. Wild-type (WT) and TauC3 mice were analyzed with a wire-hang test for their grip strength and cooperative motor function. Each group of mice was tested at 2, 3, 6, 9, and 12 months of age. Data are means ± SEM (n = 19). (B) TauC3 expression does not affect the hyperactivity or normal locomotor function in the mice. Total arm entries of wild-type (WT) and TauC3 mice in Y-maze test were counted at the indicated ages. Data are means ± SEM (n = 19).

A

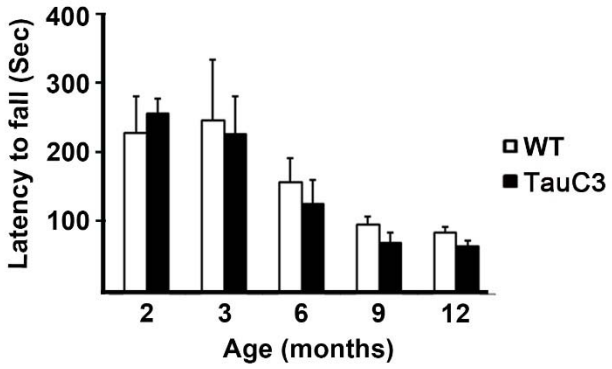
Latency to fall (Sec)
400
300
200
100
2
3
6
9
12
Age (months)
WT
TauC3

B

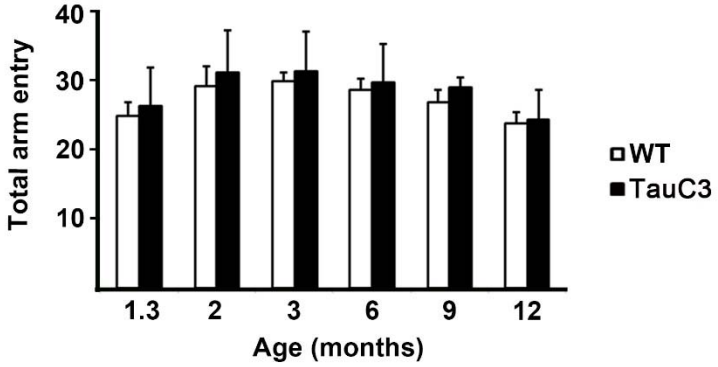
Total arm entry
40
30
20
10
1.3
2
3
6
9
12
Age (months)
WT
TauC3

Figure 1-6. Reduced synaptic proteins in the hippocampus CA3 region of TauC3 mice at young age.

(A-B) Hippocampal tissues were immunostained using synaptophysin antibody (mf) and Hoechst 33342 (py). mf; mossy fiber region, py, pyramidal region. Scale bars, 50 μm. (A) Densitometric analysis of synaptophysin (Syn) on the fluorescence in A (B). (C-D) The hippocampal tissue lysates of wild-type (WT) and TauC3 mice were examined with Western blot analysis (C) and the signals on the blot in C were quantified by densitometric analysis (D). (Bars represent means ± SEM, $*p < 0.05$, $**p < 0.005$, $n = 3$, slice = 6).

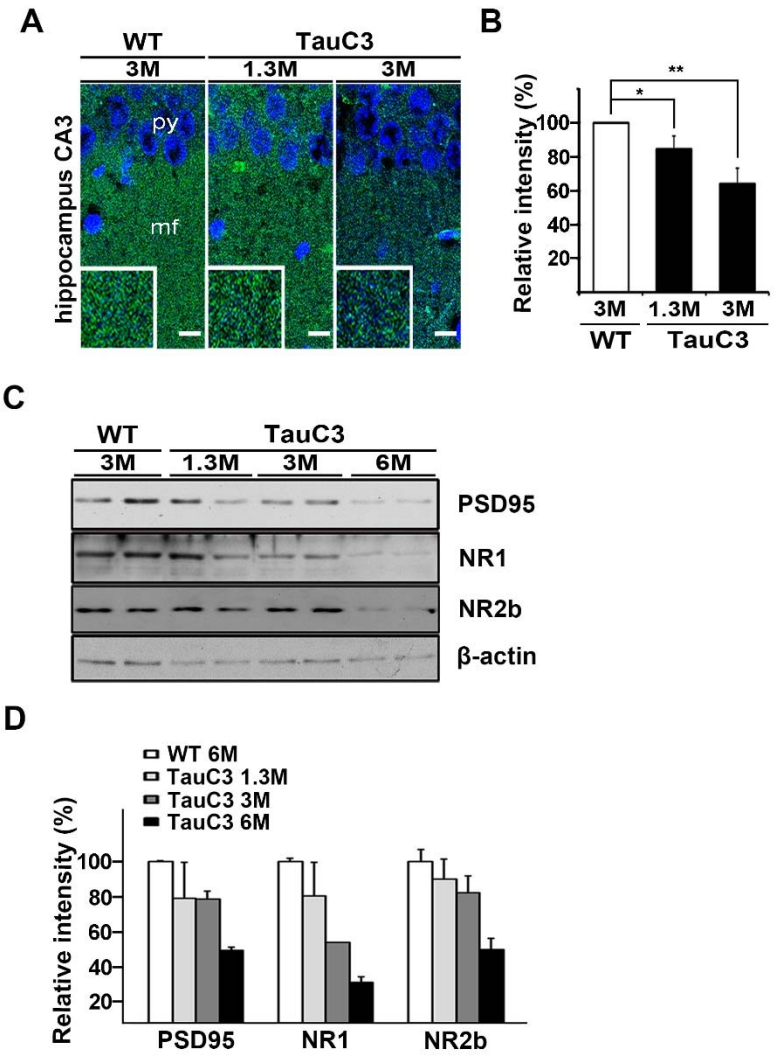
A
WT
TauC3
3M
1.3M
3M
hippocampus CA3
py
mf
B
Relative intensity (%)
**
*
100
80
60
40
20
3M
1.3M
3M
WT
TauC3
C
WT
TauC3
3M
1.3M
3M
6M
PSD95
NR1
NR2b
β-actin
D
WT 6M
TauC3 1.3M
TauC3 3M
TauC3 6M
Relative intensity (%)
100
80
60
40
20
PSD95
NR1
NR2b

Figure 1-7. Occurrence of TUNEL-positive cell death in aged TauC3 mice.

(A) The hippocampal CA3 and cortex regions of 12 month-old wild-type (WT) and 1.3, 6, and 12 month-old TauC3 mice were examined with TUNEL assay for dead cells and Hoechst dye staining (DAPI) for nuclei and then observed under fluorescence microscope. Scale bars, 50 μm. (B) The TUNEL-positive signals of the tissue slice were counted. Data are means ± SEM ($p < 0.05$, $n = 4$, slices = 12).

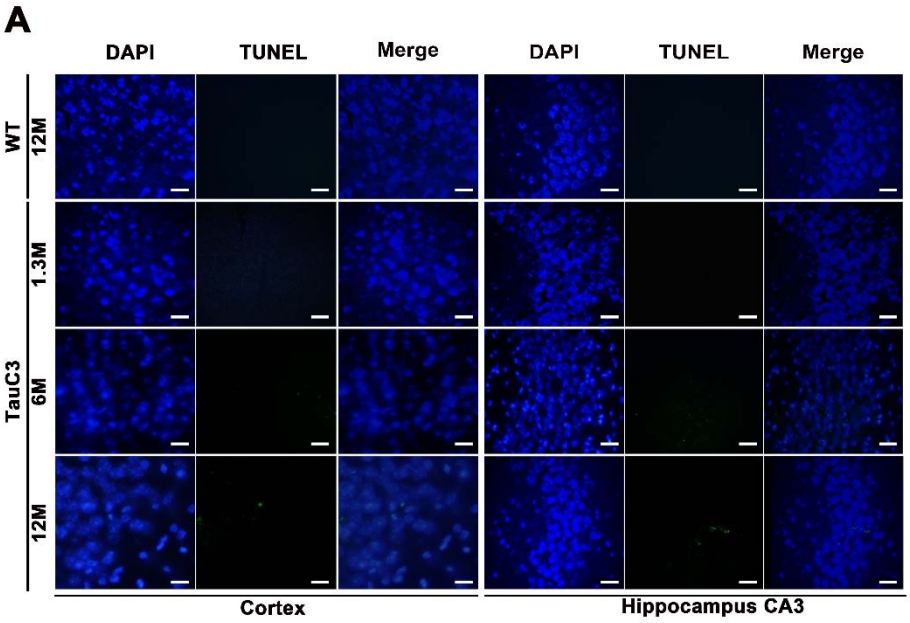
A
DAPI
TUNEL
Merge
DAPI
TUNEL
Merge
WT
12M
TauC3
1.3M
6M
12M
Cortex
Hippocampus CA3

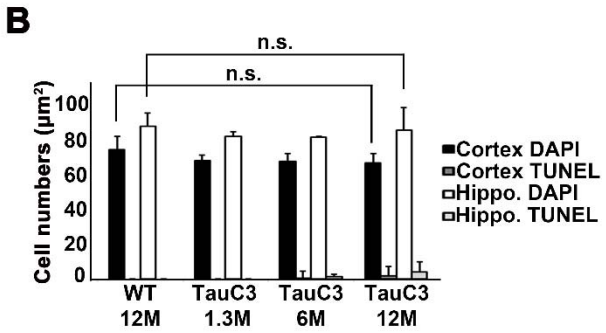
B
n.s.
n.s.
Cell numbers (μm²)
100
80
60
40
20
0
WT 12M
TauC3 1.3M
TauC3 6M
TauC3 12M
Cortex DAPI
Cortex TUNEL
Hippo. DAPI
Hippo. TUNEL

Figure 1-8. Hematoxylin staining showing cell numbers in the hippocampus and cortex.

(A) The hippocampal CA1 and CA3 and cortex regions of 12 month-old wild-type (WT) and 1.3, 3, 6, and 12 month-old TauC3 mice were stained with hematoxylin. (B) The numbers of hematoxylin-positive cells in (A) were counted. Data are means ± SEM (n = 3) (right). Scale bars, 100 μm, n.s, not significant.

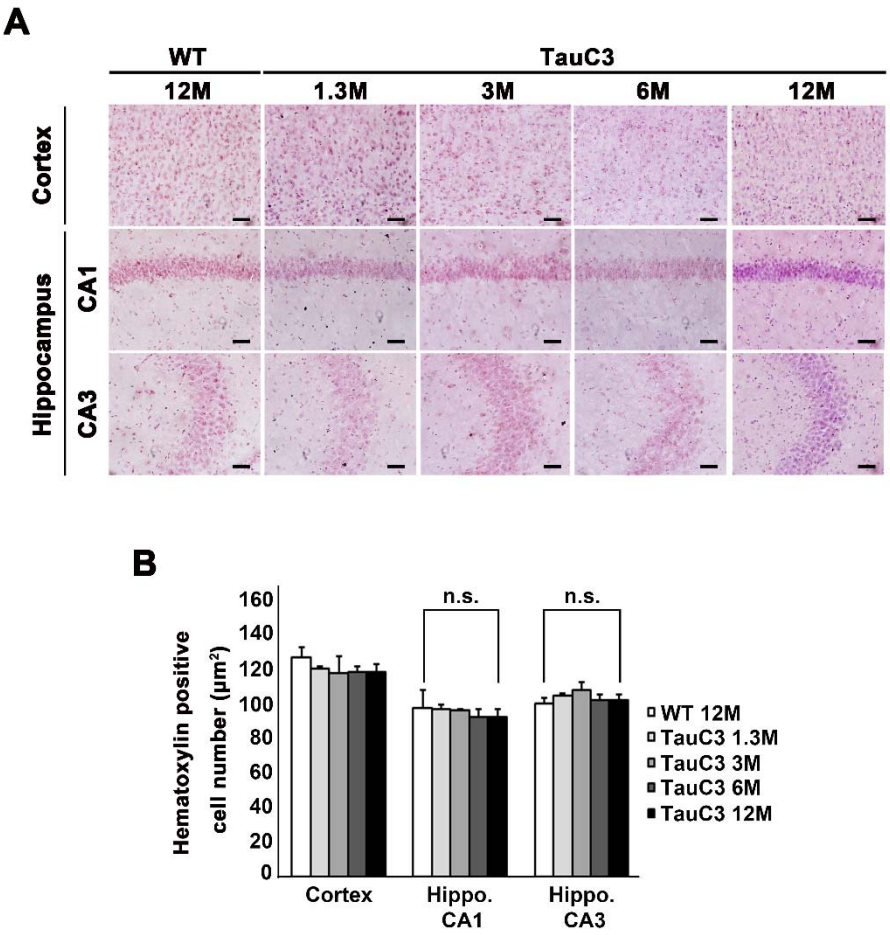
A
WT
TauC3
12M
1.3M
3M
6M
12M
Cortex
Hippocampus
CA1
CA3
B
Hematoxylin positive cell number (μm²)
160
140
120
100
80
60
40
20
0
n.s.
n.s.
Cortex
Hippo. CA1
Hippo. CA3
WT 12M
TauC3 1.3M
TauC3 3M
TauC3 6M
TauC3 12M

Figure 1-9. Lifespan analysis of TauC3 mice.

Kaplan–Meier survival curve for TauC3 mice and wild-type (WT) littermates (n = 64 for TauC3 and n = 57 for WT mice). Data are means ± SEM.

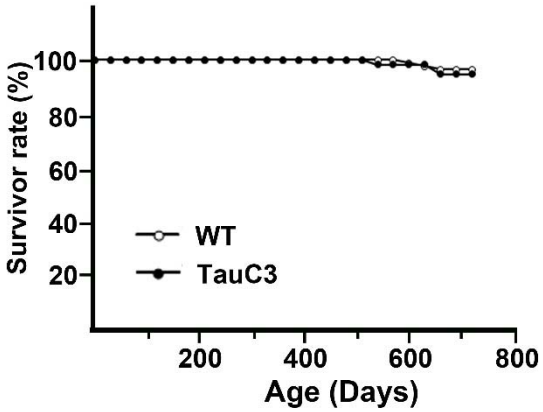
Survivor rate (%)
100
80
60
40
20
WT
TauC3
200
400
600
800
Age (Days)

Figure 1-10. Appearance of Tau hyperphosphorylation in TauC3 mice. (**A**) Hyperphosphorylation and conformational change of Tau in the hippocampus of TauC3 mice. The hippocampal tissue lysates prepared from wild-type (WT) and TauC3 mice were examined with Western blotting. (**B**) The signals on the blot in (A) were quantified by densitometric analysis. Bars represent means ± SEM (n = 3).

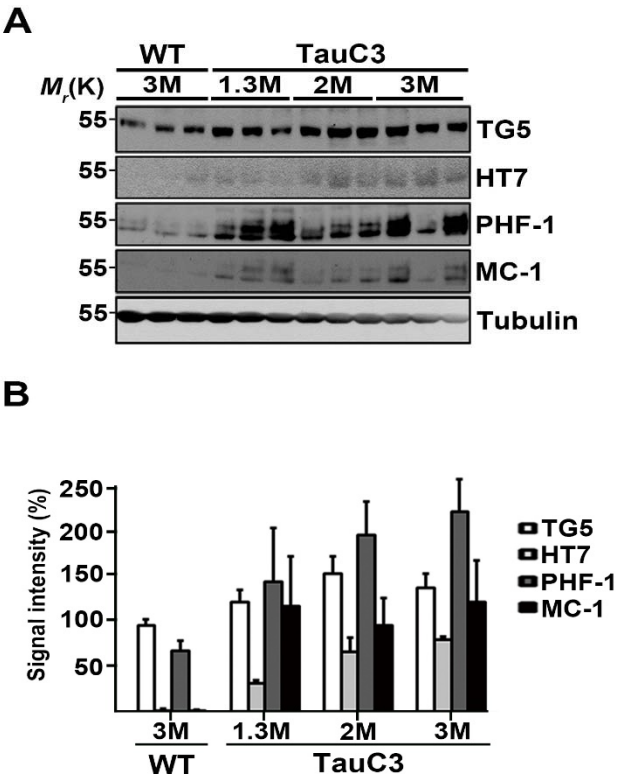
A
WT
TauC3
M_r(K)
3M
1.3M
2M
3M
55
TG5
HT7
PHF-1
MC-1
Tubulin
B
Signal intensity (%)
250
200
150
100
50
TG5
HT7
PHF-1
MC-1
3M
1.3M
2M
3M
WT
TauC3

Figure 1-11. Detection of high molecular weight of Tau oligomers in TauC3 mice.

(A) Effects of reducing agents on the formation of 170 kDa Tau oligomers. TauC3 brain extracts were incubated with or without beta-mercaptoethanol and/or DTT as indicated and then analyzed with Western blot analysis. (B) Hippocampal tissue lysates dissolved in non-reducing sample buffer were analyzed with Western blotting using the indicated antibodies. Arrows, Tau oligomers; arrowhead, monomeric Tau; n.s., nonspecific signal. (C) The signals on the blot B were quantified by densitometric analysis. Bars represent means ± SEM (n = 3). (D) The hippocampal tissue lysates prepared from 2 and 9 month-old wild type (WT), TauC3, and 3X TG mice were analyzed with Western blotting under non-reducing condition. n.s., non-specific signal.

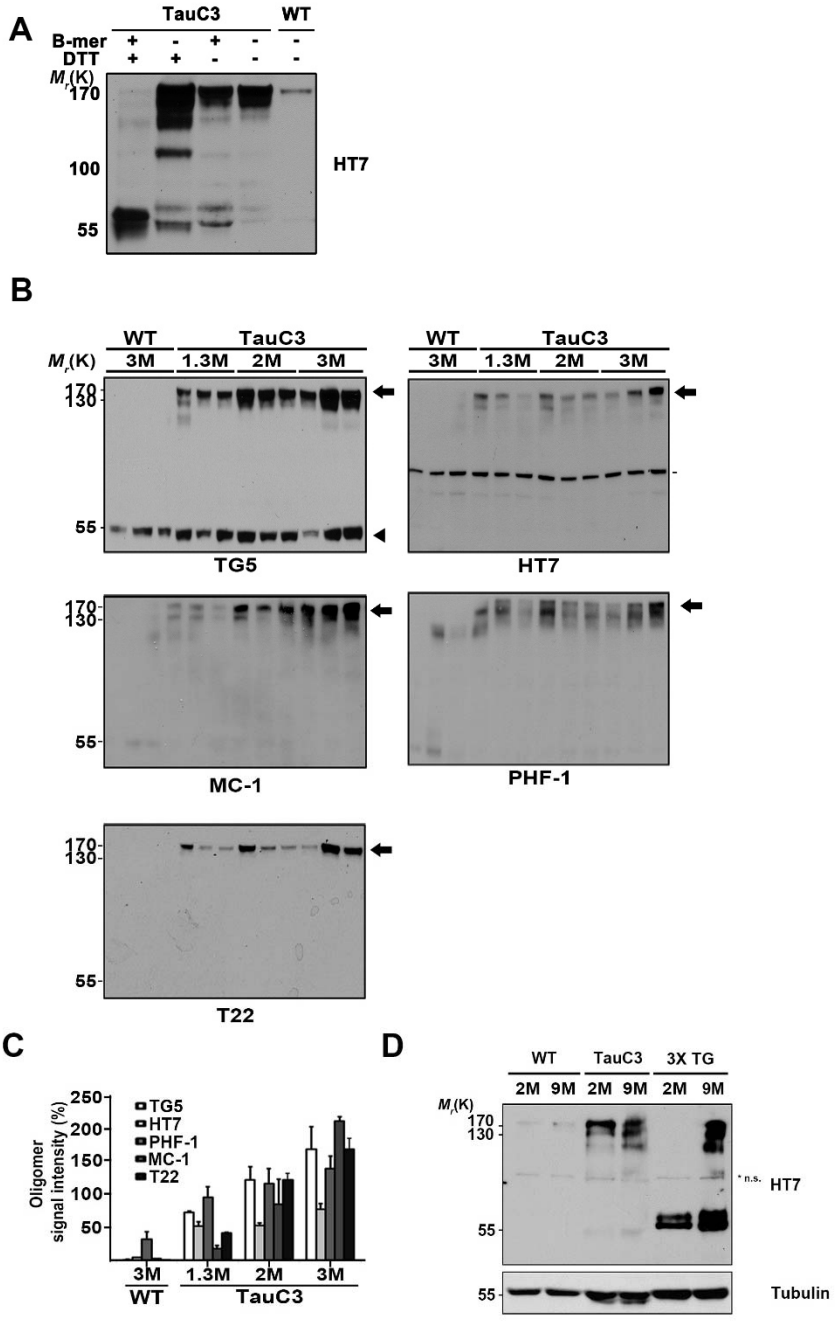
A
TauC3
WT
B-mer
DTT
M_r(K)
170
100
55
HT7
B
WT
TauC3
3M
1.3M
2M
3M
170
130
55
TG5
HT7
MC-1
PHF-1
T22
C
Oligomer signal intensity (%)
250
200
150
100
50
TG5
HT7
PHF-1
MC-1
T22
3M
1.3M
2M
3M
WT
TauC3
D
WT
TauC3
3X TG
2M
9M
M_r(K)
170
130
55
n.s.
HT7
Tubulin

Figure 1-12. Immunohistochemical analysis showing Tau oligomers in the hippocampal tissue of TauC3 mice.

The CA3 region of the hippocampus of 6 month-old wild-type (WT) and 3 and 6 month-old TauC3 mice were analyzed with immunohistochemistry using the indicated antibodies: HT7, PHF-1, MC1, T22. Scale bars, 100 μm.

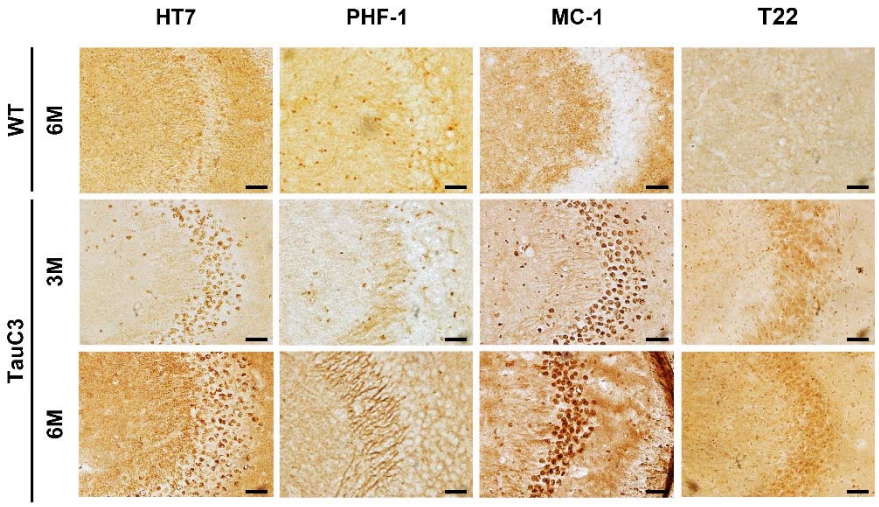
HT7
PHF-1
MC-1
T22
WT
6M
TauC3
3M
6M

Figure 1-13. The treatment with Aβ oligomers induces the formation of T22-positive tau oligomers in a caspase-dependent manner in cultured neurons.

(A, B) Primary cortical neurons at DIV 14 were transfected with pEGFP, pEGFP-Tau, or pEGFP-TauC3 for 24 hr and then left untreated or treated with 5 μM Aβ in the presence or absence of 20 μM caspase-3 inhibitor (z-DEVD-fmk) for another 12 hr. The neurons were observed under fluorescence microscope. Scale bars, 10 μm (A, upper). The spine density of the neurons was examined by densitometric analysis. Bars represent means ± SEM (***$p < 0.001$, *$p < 0.05$) (A, lower). In addition, the treated neurons were immunostained with T22 antibody (red) and observed under fluorescence microscope (green for GFP). Scale bars, 50 μm (B).

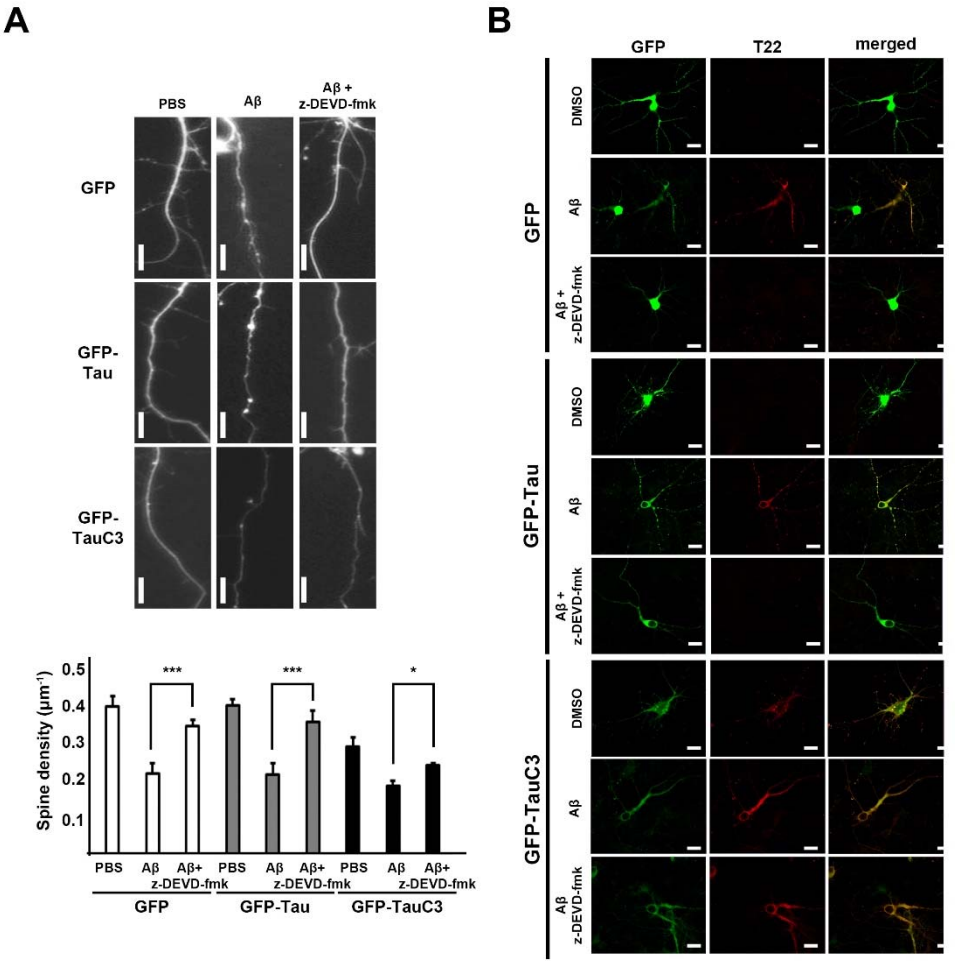
A
PBS
Aβ
Aβ + z-DEVD-fmk
GFP
GFP-Tau
GFP-TauC3
Spine density (μm⁻¹)
0.5
0.4
0.3
0.2
0.1
***
***
*
PBS
Aβ
Aβ+ z-DEVD-fmk
GFP
GFP-Tau
GFP-TauC3
B
GFP
T22
merged
DMSO
Aβ
Aβ + z-DEVD-fmk
GFP
GFP-Tau
GFP-TauC3

Figure 1-14. Caspase inhibitor blocks Tau cleavage and oligomer formation, and attenuates memory deficit in the Aβ oligomers-injected mice.

(A) Experimental scheme of Aβ oligomer injection and memory test. Wild-type (WT) at 6 months were *i.c.v.*-injected with PBS, caspase inhibitor IDN-6556 (1 mM), or Aβ oligomers (15 μg) alone or together with caspase inhibitor IDN6556, as indicated. (B) Aβ oligomer injection induces memory impairment in a caspase-dependent manner. Spatial memory of each group (n = 7 - 8) of the mice was measured at 2 days after the injection. Bars represent means ± SEM (*$p < 0.05$). (C) Immunohistochemical analysis showing TauC3 and Tau oligomers in the hippocampus and cortex of the Aβ oligomer-injected mice. The hippocampus (CA1 region) and the cortex were prepared at 7 days after the injection and analyzed with immunohistochemistry using TauC3, T22, and AT8 antibodies. The same brain regions of 9-month old 3X-TG mice were used as controls. Scale bars, 100 μm.

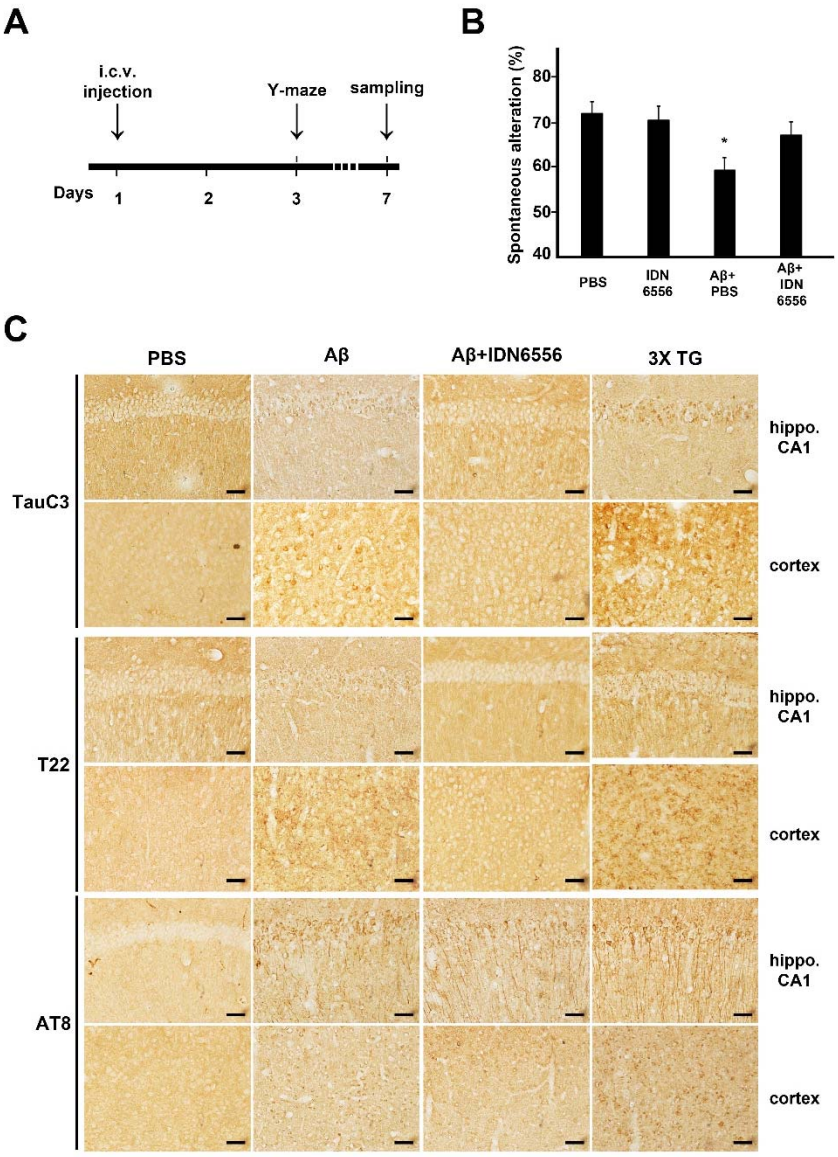
A
i.c.v. injection
Y-maze
sampling
Days
1
2
3
7
B
Spontaneous alteration (%)
80
70
60
50
40
*
PBS
IDN 6556
Aβ+ PBS
Aβ+ IDN 6556
C
PBS
Aβ
Aβ+IDN6556
3X TG
TauC3
T22
AT8
hippo. CA1
cortex

Figure 1-15. Detection of detergent (NP-40)-insoluble Tau aggregates in TauC3 mouse brain. (A)Wild-type (WT) and TauC3 hippocampal tissue lysates insoluble in RIPA buffer containing 0.5 % NP-40 were analyzed with Western blotting. (B) The signals on the blot (A) were quantified by densitometric analysis. Bars represent the relative ratio of NP-40-insoluble Tau (n = 3). (C) Tissue extracts of the hippocampus were analyzed with filter trap assay. (D) The signals on the blots of filter trap assay in (A) were quantified by densitometric analysis. Data are means ± SEM (n = 3).

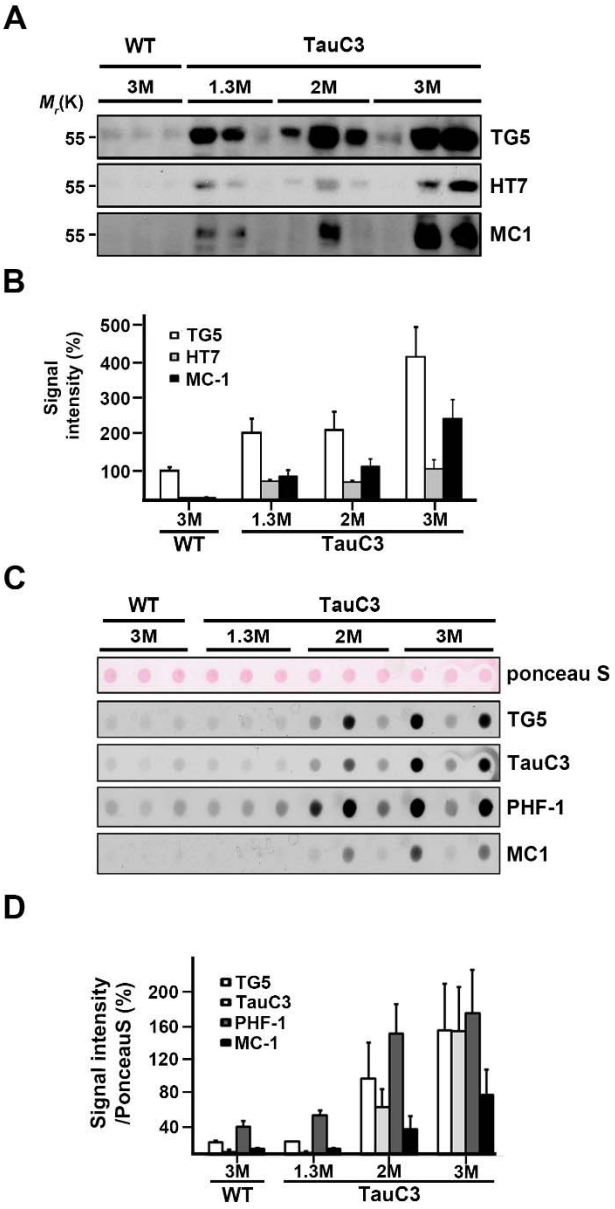
A
WT
TauC3
3M
1.3M
2M
3M
M_r(K)
55
TG5
55
HT7
55
MC1
B
Signal intensity (%)
500
400
300
200
100
TG5
HT7
MC-1
3M
1.3M
2M
3M
WT
TauC3
C
WT
TauC3
3M
1.3M
2M
3M
ponceau S
TG5
TauC3
PHF-1
MC1
D
Signal intensity /PonceauS (%)
200
160
120
80
40
TG5
TauC3
PHF-1
MC-1
3M
1.3M
2M
3M
WT
TauC3

Figure 1-16. **Detection of silverstainig positive Tau aggregates with filamentous structure in TauC3 mice.**

(A) Silver staining-positive tangle formation in the Layer I and II of the cortex and the CA3 region of the hippocampal tissue of TauC3 mice. Scale bars, 50 μm. (B) The 0.5% NP-40-insoluble hippocampal lysates were subjected to immunoprecipitation assay with Tau3 antibody cross-linked to protein A-beads. The immunoprecipitates and Tau aggregates which were prepared from purified Tau protein in the presence of heparin were observed by TEM. Scale bars, 100 nm.

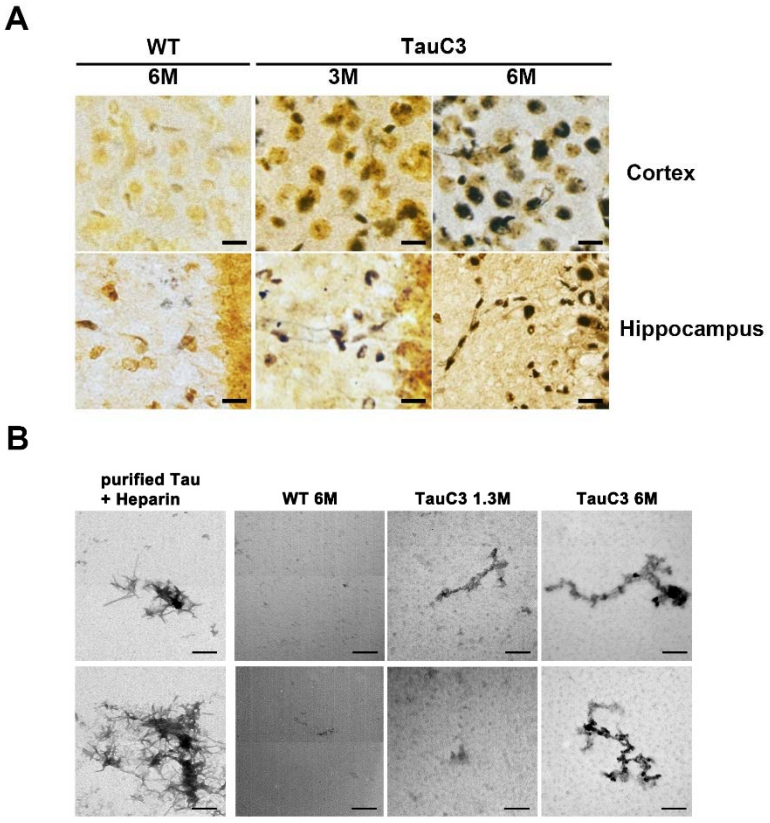
A
WT
TauC3
6M
3M
6M
Cortex
Hippocampus
B
purified Tau
+ Heparin
WT 6M
TauC3 1.3M
TauC3 6M

Figure 1-17. Effects of methylene blue and Congo red on the filament formation of Tau protein *in vitro* and in cell model.

(A) Purified Tau protein (10 μM) was incubated with heparin (20 μM) in the absence or presence of methylene blue (10 μM) or Congo red (10 μM). After being added with thioflavin T (25 μM), the reaction mixtures were measured for the absorbance with spectrofluorometer. (B) SH-SY5Y cells were transfected with GFP-Tau alone or together with GSK3 for 16 h, after which cells were left untreated or treated with 20 mM LiCl, 3 μM (*left panels*) or 5 μM, (*right panels*) doses of methylene blue (MB) and Congo red (CR) for additional 30 h. Cell lysates were analyzed with Western blotting (WB) and filter trap assays.

A

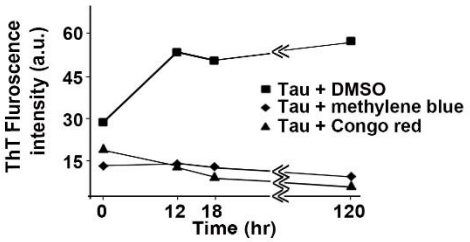
ThT Fluroscence intensity (a.u.)
60
45
30
15
0
12
18
120
Time (hr)
Tau + DMSO
Tau + methylene blue
Tau + Congo red

B

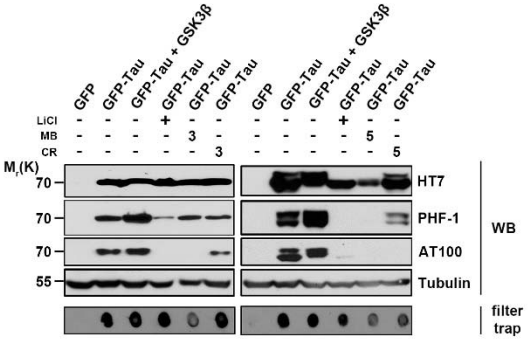
GFP
GFP-Tau
GFP-Tau + GSK3β
GFP-Tau
GFP-Tau
GFP-Tau
LiCl
MB
CR
M_r(K)
70
70
70
55
HT7
PHF-1
AT100
Tubulin
WB
filter trap

Figure 1-18. *i.p.* injection of Methylene blue or *i.c.v.* injection of Congo red retards the memory impairment in TauC3 mice.

(A-C) Experimental scheme of drug treatments and memory tests. Wild-type (WT) and TauC3 mice at one month of age were *i.p.*-injected with Methylene blue(10 mg/kg/day) for 30 days or biweekly *i.c.v.*-injected with Congo red (75 μg). Spatial memory of TauC3 mice was measured twice at 1.3 months (10 days after injection) and 2 months (30 days after injection) of age and recognition memory was at 2 months of age (A). The mice were then examined for spatial memory with a Y-maze test (B) and recognition memory with a novel recognition test (C). Values are means ± SEM. (*p = 0.083, **p = 0.015, ***p =0.0051, n = 11~18).

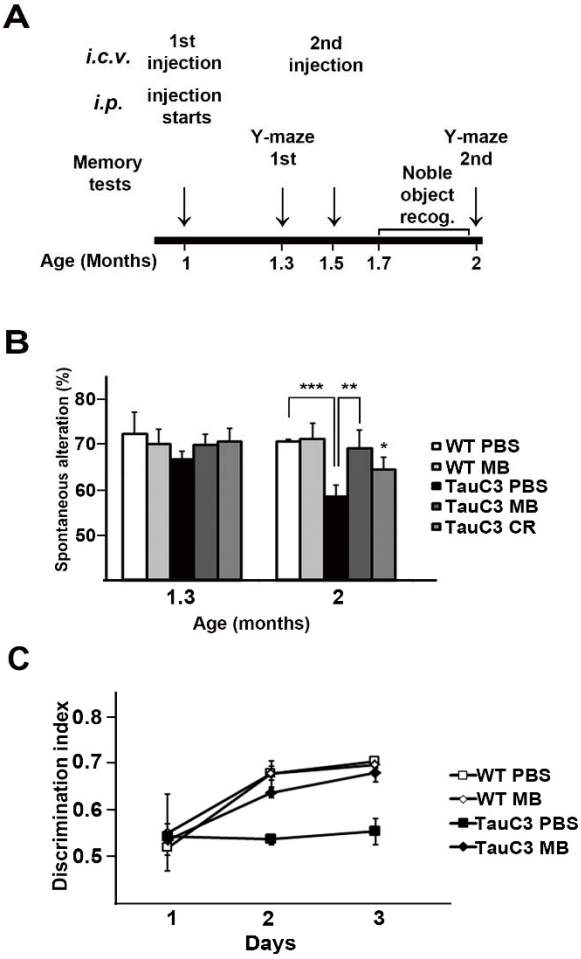
A
i.c.v.
1st injection
2nd injection
i.p.
injection starts
Memory tests
Y-maze 1st
Y-maze 2nd
Noble object recog.
Age (Months)
1
1.3
1.5
1.7
2
B
Spontaneous alteration (%)
80
70
60
50
***
**
*
WT PBS
WT MB
TauC3 PBS
TauC3 MB
TauC3 CR
1.3
2
Age (months)
C
Discrimination index
0.8
0.7
0.6
0.5
WT PBS
WT MB
TauC3 PBS
TauC3 MB
1
2
3
Days

Figure 1-19. Memory impairment of TauC3 mice is not attenuated by *i.p.*-injection of Congo red.

Wild-type (WT) and TauC3 mice were examined for spatial memory with a Y-maze test at 2 months of age. Bars and values represent means ± SEM (***$p < 0.005$).

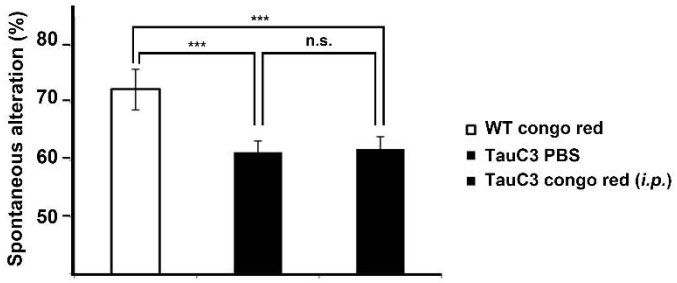
Spontaneous alteration (%)
80
70
60
50
***
***
n.s.
WT congo red
TauC3 PBS
TauC3 congo red (i.p.)

Figure 1-20. Methylene blue decreases the amounts of 170kDa Tau oligomers.

The hippocampal tissue lysates dissolved in non-reducing sample buffer were analyzed with Western blotting under non-reducing condition. Arrows, Tau oligomers; arrowhead, Tau monomer; n.s., nonspecific signal.

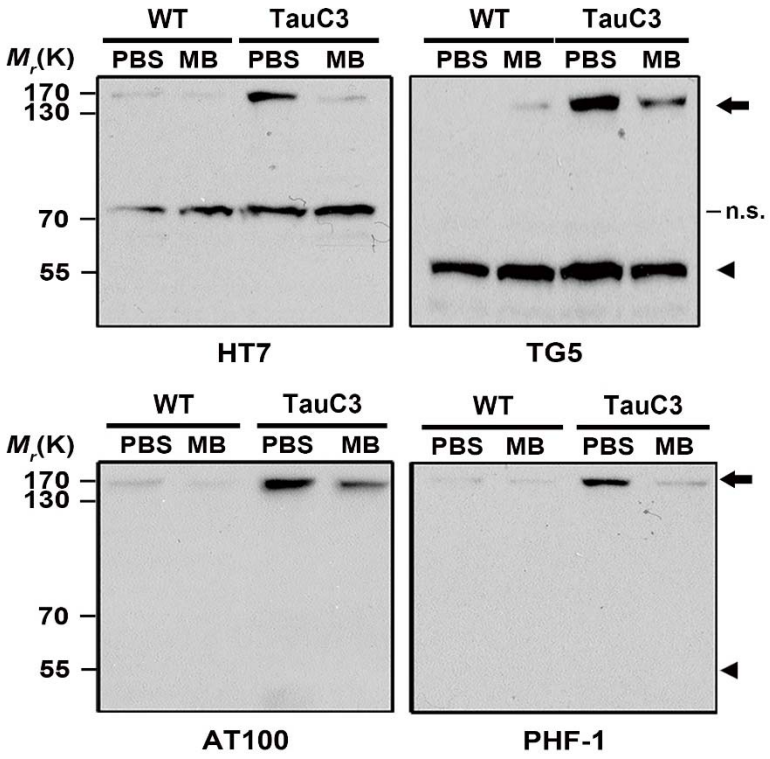
WT
TauC3
WT
TauC3
M_r(K)
PBS MB PBS MB
PBS MB PBS MB
170
130
70
55
n.s.
HT7
TG5
WT
TauC3
WT
TauC3
M_r(K)
PBS MB PBS MB
PBS MB PBS MB
170
130
70
55
AT100
PHF-1

Figure 1-21. Methylene blue preferentially decreases the amounts of TauC3 and PHF-1-positive tau.

The hippocampal tissues were analyzed with Western blotting under reducing condition. The amount of total Tau (TG5) was a little changed by methylene blue, whereas TauC3 (HT7) and PHF-1 Tau were reduced.

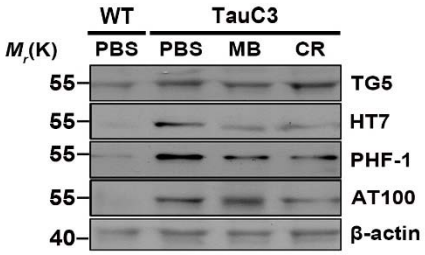
WT
TauC3
M_r(K)
PBS
PBS
MB
CR
55
TG5
55
HT7
55
PHF-1
55
AT100
40
β-actin

Figure 1-22. Immunohistochemical analysis showing the decrease of human TauC3 and tau oligomers by methylene blue in TauC3 mice.

The CA3 regions of wild-type (WT) and TauC3 mice used in Fig. 6 were examined with immunohistochemical analysis using HT7 and T22 antibodies. Scale bars, 100 μm.

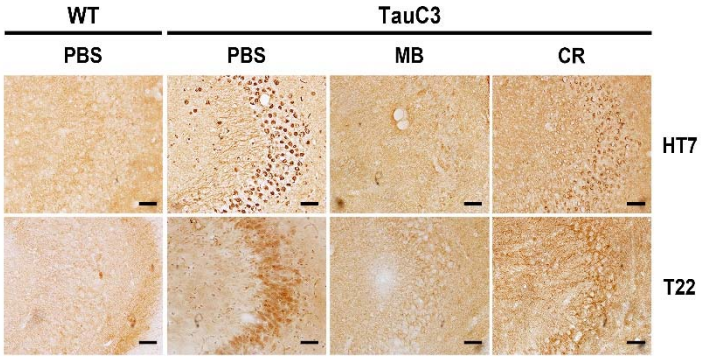
WT
TauC3
PBS
PBS
MB
CR
HT7
T22

Figure 1-23. Methylene blue rescues the loss of spine density and synaptic proteins in TauC3 overexpressed primary neuron and TauC3 mice.

(A) Cultured hippocampal neurons (DIV 13) were transfected with GFP, GFP-tau, GFP-TauC3, or both GFP-tau and GFP-TauC3, after which cells were left untreated or treated with 50 nM methylene blue (MB) for 24 h. Scale bars, 10 μm. (B) The signals on the blots of filter trap assay in (A) were quantified by densitometric analysis. Data are means ± SEM (n = 3). (C) Wild-type (WT) and TauC3 mice (1 month of age) were daily *i.p.*-injected with PBS or methylene blue (MB, 10 mg/kg/day) for 30 days. The hippocampal tissue lysates were prepared and examined with Western blot analysis using PSD95, NR1, and β-actin antibodies.

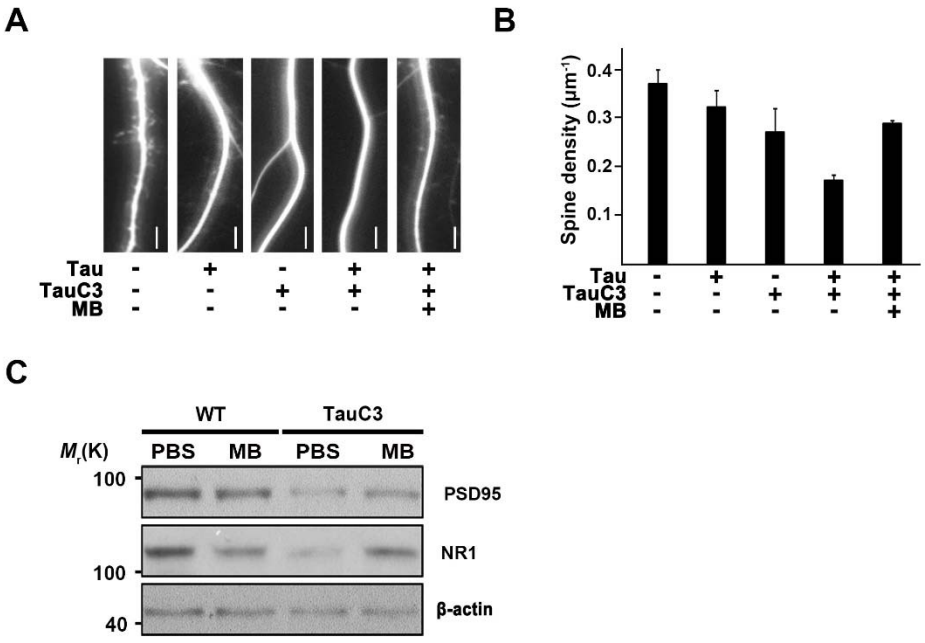
A
Tau - + - + +
TauC3 - - + + +
MB - - - - +
B
Spine density (μm-1)
0.4
0.3
0.2
0.1
Tau - + - + +
TauC3 - - + + +
MB - - - - +
C
WT
TauC3
Mr(K)
PBS
MB
PBS
MB
100
PSD95
NR1
100
40
β-actin

Figure 1-24. Rapamycin rescues the spatial and recognition memory impairment in TauC3 mice.

(A) Wild-type (WT) and TauC3 mice were daily *i.p.*-injected from one month of age for 30 days with rapamycin (10 mg/kg). Spatial memory was measured twice at 1.3 months (10 days after injection) and 2 months (30 days after injection) of age. (B) recognition memory was measured at 2 months of age. Data are means ± SEM (**p = 0.0026, ***p = 0.0018 n = 11~18).

A

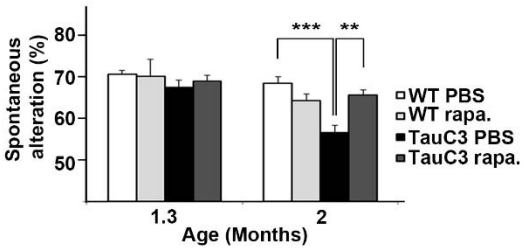
Spontaneous alteration (%)
80
70
60
50
***
**
1.3
2
Age (Months)
WT PBS
WT rapa.
TauC3 PBS
TauC3 rapa.

B

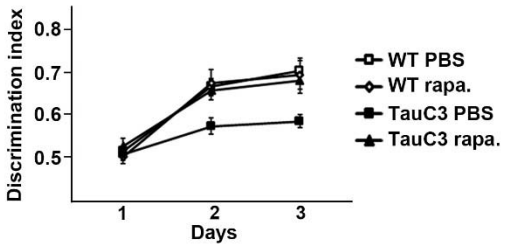
Discrimination index
0.8
0.7
0.6
0.5
1
2
3
Days
WT PBS
WT rapa.
TauC3 PBS
TauC3 rapa.

Figure 1-25. Reduction of the phosphorylated tau and detergent-insoluble tau aggregates by rapamycin in TauC3 mice. Hippocampal tissues examined in (1-35) were analyzed with Western blotting fractionated into RAB-soluble, RIPA-soluble and -insoluble (70% FA-soluble) fractions for Western blotting.

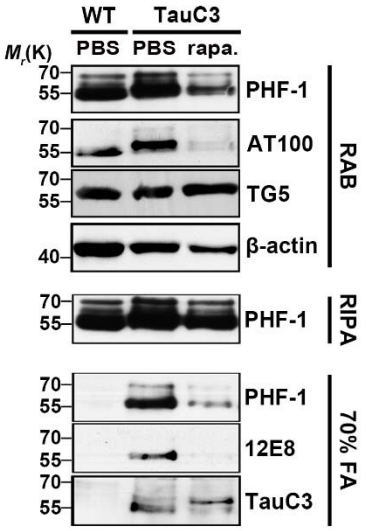
WT
TauC3
PBS
PBS
rapa.
M_r(K)
70
55
PHF-1
AT100
TG5
40
β-actin
RAB
RIPA
12E8
TauC3
70% FA

Figure 1-26. **Enhanced autophagy markers in the rapamycin-treated hippocampal tissues of TauC3 mice.**

Western blot is analyzed with LC3, p62and p-S6 antibodies for rapamycin induced autophagy related protein change.

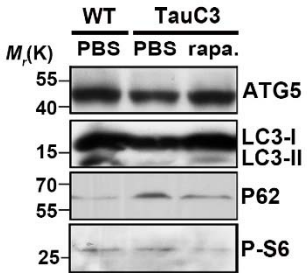
WT
TauC3
PBS
PBS
rapa.
M_r(K)
55
40
15
70
55
25
ATG5
LC3-I
LC3-II
P62
P-S6

Figure 1-27. **Effect of rapamycin on the level of tau oligomers in TauC3 mice.**

The hippocampal tissues examined in Figure 1-36 were analyzed with Western blotting under non-reducing condition. Arrows, tau oligomers; arrowhead, tau monomer; n.s., nonspecific signal.

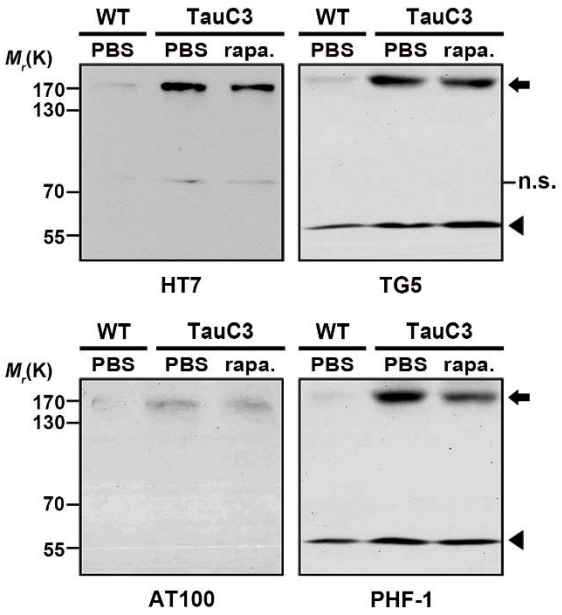
WT
TauC3
WT
TauC3
PBS
PBS
rapa.
PBS
PBS
rapa.
M_r(K)
170
130
70
55
n.s.
HT7
TG5
WT
TauC3
WT
TauC3
PBS
PBS
rapa.
PBS
PBS
rapa.
M_r(K)
170
130
70
55
AT100
PHF-1

DISCUSSION

Because of their association with toxicity, the roles of soluble oligomers and insoluble aggregates of disease-associated proteins have received considerable attention in many neurodegenerative diseases, such as Aβ and Tau oligomers in AD, Huntingtin oligomers in Huntington's disease, and α-synuclein oligomers in Parkinson's disease (Haass and Selkoe, 2007). However, the presence and role of Tau oligomers and aggregates in animal models and AD pathogenesis are still poorly understood. TauC3 mice containing an oligomeric form of Tau show a strong association with memory deficits. In this mouse, detergent (0.5% NP-40)-soluble high molecular weight (around 170 kDa) of Tau was observed under a non-reducing condition. Similar sizes of Tau oligomers with approximately 130–200 kDa (Flach et al., 2012), 140–170 kDa (Berger et al., 2007), 150 kDa (Sahara et al., 2007), and 180 kDa (Patterson et al., 2011) were also previously detected with *in vitro* assays and in the brain of AD patients. Especially, compared to existing Tau mouse models, TauC3 in TauC3 mice was detected mainly in its oligomeric form, detected by Tau oligomer-specific antibody, T22. Because TauC3 was reported to possess enhanced ability to assemble filament *in vitro* (Gamblin

et al., 2003), TauC3 may form a self-oligomer or act as a seed to increase oligomers with endogenous mouse Tau (Rissman et al., 2004). While whether 170 kDa Tau was a dimer or trimer was not clear, Tau low-n oligomers and aggregates appeared in TauC3 mice at an early age (1.3 months), which coincides with the onset of memory impairment in TauC3 mice.

While TauC3 increases Tau phosphorylation and facilitates oligomer formation in the transgenic mice, the mechanism by which TauC3 affects memory impairment is currently unclear. The most prominent factor for the memory deficits observed in TauC3 mice may be TauC3 itself. According to our results, TauC3 evokes neurite regression and reduces synaptic density in cultured neurons and TauC3 mice. Consistently, methylene blue or rapamycin enhances memory function in TauC3 mice and increases synaptic density in primary neurons expressing Tau and TauC3. It appears that TauC3 exerts detrimental effects on synaptic density for memory loss. In addition, other groups have reported that TauC3 decreases mitochondria membrane potential and inhibits axonal transport, which leads to reduced synaptic button formation in cultured neurons (Quintanilla et al., 2009). Additionally, injection of a 120–170 kDa synthetic Tau oligomers or an AD brain-derived 110–160 kDa Tau oligomers into mice has been shown to decrease synaptophysin density (Lasagna-Reeves et al., 2011) and reduce hippocampal

long-term potentiation for memory impairment (Lasagna-Reeves et al., 2012). Thus, the synaptic dysfunction observed in TauC3 mice is attributed to TauC3 oligomerization.

While electronmicroscope-detectable Tau filaments are found from 1.3 month of age, increasing up to 6 months, and silver staining-positive Tau aggregates were first found at 3 months in TauC3 mice, TUNEL-positive cell death was not observed until 6 month of age. TUNEL-positive cell death was barely detected at late stage in older TauC3 mice showing severe memory impairment. Thus, compared to wild-type mice, there was no visible reduction in total cell numbers in the affected tissues of TauC3 mice. Like TauC3, many AD model mice, including TG2576 mice and Tau P301L mice, do not always show visible neuronal loss in the cortex and hippocampus despite apparent memory loss (Chapman et al., 1999; Lewis et al., 2000). Similarly, in 24 month-old TauΔK280 TG mice, silver staining-positive Tau aggregates have been observed without significant neuronal loss (Terwel et al., 2005). Calignon *et al.* also observed caspase activation in the brains of rTG4510 mice and concomitant fast tangle formation without cell death in neurons within tangles (de Calignon et al., 2010). While detergent-insoluble Tau increases in TUNEL-positive cells in TauC3 model of *D. melanogaster* (Khurana et al., 2010), I believe that neuronal loss or cell death remains very

limited in TauC3 mice.

Most striking finding in this study is that TauC3 mice exhibit memory deficits as early as at 2 months of age. This is compared to a non-mutated form of Tau, which usually leads to memory deficits in aged mice (> 9–18 month) (Duff et al., 2000; Gotz et al., 1995) and to Tau P301L, a FTDP-17 familiar Tau mutant that leads to memory deficits at 6 months (Terwel et al., 2005). Though rTG4510 mice expressing Tau P301L show early memory deficits as in TauC3 mice, the expression level of Tau P301L is very high (> 13-fold of endogenous mouse Tau). In this model, 9-fold overexpression of Tau P301L does not affect memory function (Santacruz et al., 2005). On the contrary, early memory deficits in TauC3 mice are not due to TauC3 overexpression, since the expression of TauC3 is less than endogenous mouse Tau. It is also unlikely that the regional expression pattern of TauC3 driven by the promoter *BAI1-AP4* plays an unexpected role, as TauC3 mice did not show other functional deficits, involving motor coordination that is typically linked to the striatum or cerebellum. The main factor responsible for the rapid memory deficit in TauC3 mice might be Tau oligomers which appear at young age.

In the same context, methylene blue potently inhibited the formation of Tau oligomers and Tau aggregates and rescued memory impairment in

TauC3 mice, though the data regarding the role of methylene blue is somewhat controversial (Hosokawa et al., 2012; O'Leary et al., 2010). In cell culture and TauC3 mice, it appears that methylene blue functions to decrease the amount of TauC3 oligomers and aggregates at low and non-toxic dose. On the other hand, it can also affect the amount of total Tau as well as Tau oligomers. Additionally, TauC3 mice were suitable to test the inhibitory effect of rapamycin on the memory impairment, as similarly tested in other Tau mice (Caccamo et al., 2010). Bearing in mind that the onset and duration of memory decline in other Tau mouse models occurs usually much later and take longer time, rapid loss of memory in TauC3 mice will help analyzing the effects of drug candidates on AD pathogenesis early on, as seen in our assays in which twice *i.c.v.* injection or short period of *i.p.* injection was enough for the assay.

Taken together, TauC3 mice showed drastic memory impairment at an early age, associated with the appearance of Tau oligomers and aggregates. The memory impairment was remarkably rescued by drug candidate, which interfered with the formation of Tau oligomers and Tau aggregates and Tau level in the mice. I propose that TauC3 mice would be useful for analyzing Tau-associated memory loss in AD.

REFERENCES

Berger, Z., Roder, H., Hanna, A., Carlson, A., Rangachari, V., Yue, M., Wszolek, Z., Ashe, K., Knight, J., Dickson, D., *et al.* (2007). Accumulation of pathological tau species and memory loss in a conditional model of tauopathy. The Journal of neuroscience : the official journal of the Society for Neuroscience *27*, 3650-3662.

Bove, J., Martinez-Vicente, M., and Vila, M. (2011). Fighting neurodegeneration with rapamycin: mechanistic insights. Nature reviews Neuroscience *12*, 437-452.

Braak, H., and Braak, E. (1991). Neuropathological stageing of Alzheimer-related changes. Acta Neuropathol *82*, 239-259.

Caccamo, A., Majumder, S., Richardson, A., Strong, R., and Oddo, S. (2010). Molecular Interplay between Mammalian Target of Rapamycin (mTOR), Amyloid-beta, and Tau EFFECTS ON COGNITIVE IMPAIRMENTS. Journal of Biological Chemistry *285*, 13107-13120.

Chapman, P. F., White, G. L., Jones, M. W., Cooper-Blacketer, D., Marshall, V. J., Irizarry, M., Younkin, L., Good, M. A., Bliss, T. V., Hyman, B. T., *et al.* (1999). Impaired synaptic plasticity and learning in aged amyloid precursor protein transgenic mice. Nature neuroscience *2*, 271-276.

Chung, C. W., Song, Y. H., Kim, I. K., Yoon, W. J., Ryu, B. R., Jo, D. G., Woo, H. N., Kwon, Y. K., Kim, H. H., Gwag, B. J., *et al.* (2001). Proapoptotic effects of tau cleavage product generated by caspase-3. Neurobiology of disease *8*, 162-172.

de Calignon, A., Fox, L. M., Pitstick, R., Carlson, G. A., Bacskai, B. J., Spires-Jones, T. L., and Hyman, B. T. (2010). Caspase activation precedes and leads to tangles. Nature *464*, 1201-1204.

Delobel, P., Lavenir, I., Fraser, G., Ingram, E., Holzer, M., Ghetti, B., Spillantini, M. G., Crowther, R. A., and Goedert, M. (2008). Analysis of tau phosphorylation and truncation in a mouse model of human tauopathy. Am J Pathol *172*, 123-131.

Duff, K., Knight, H., Refolo, L. M., Sanders, S., Yu, X., Picciano, M., Malester, B., Hutton, M., Adamson, J., Goedert, M., *et al.* (2000). Characterization of pathology in transgenic mice over-expressing human genomic and cDNA tau transgenes. Neurobiology of disease *7*, 87-98.

Flach, K., Hilbrich, I., Schiffmann, A., Gartner, U., Kruger, M., Leonhardt, M., Waschipky, H., Wick, L., Arendt, T., and Holzer, M. (2012). Tau oligomers impair artificial membrane integrity and cellular viability. The Journal of biological chemistry *287*, 43223-43233.

Gabbita, S. P., Scheff, S. W., Menard, R. M., Roberts, K., Fugaccia, I., and Zemlan, F. P. (2005). Cleaved-tau: a biomarker of neuronal damage after traumatic brain injury. Journal of neurotrauma *22*, 83-94.

Gamblin, T. C., Chen, F., Zambrano, A., Abraha, A., Lagalwar, S., Guillozet, A. L., Lu, M., Fu, Y., Garcia-Sierra, F., LaPointe, N., *et al.* (2003). Caspase cleavage of tau: linking amyloid and neurofibrillary tangles in Alzheimer's disease. Proceedings of the National Academy of Sciences of the United States of America *100*, 10032-10037.

Gotz, J., Probst, A., Spillantini, M. G., Schafer, T., Jakes, R., Burki, K., and Goedert, M. (1995). Somatodendritic localization and hyperphosphorylation of tau protein in transgenic mice expressing the longest human brain tau isoform. The EMBO journal *14*, 1304-1313.

Gravitz, L. (2011). DRUGS A tangled web of targets. Nature *475*, S9-S11.

Guillozet-Bongaarts, A. L., Garcia-Sierra, F., Reynolds, M. R., Horowitz, P. M., Fu, Y., Wang, T., Cahill, M. E., Bigio, E. H., Berry, R. W., and Binder, L. I. (2005). Tau truncation during neurofibrillary tangle evolution in Alzheimer's disease. Neurobiology of aging *26*, 1015-1022.

Haass, C., and Selkoe, D. J. (2007). Soluble protein oligomers in neurodegeneration: lessons from the Alzheimer's amyloid beta-peptide. Nature reviews Molecular cell biology *8*, 101-112.

Hanger, D. P., Brion, J. P., Gallo, J. M., Cairns, N. J., Luthert, P. J., and Anderton, B. H. (1991). Tau in Alzheimer's disease and Down's syndrome is insoluble and abnormally phosphorylated. The Biochemical journal *275 (Pt 1)*, 99-104.

Hosokawa, M., Arai, T., Masuda-Suzukake, M., Nonaka, T., Yamashita, M., Akiyama, H., and Hasegawa, M. (2012). Methylene blue reduced abnormal tau accumulation in P301L tau transgenic mice. PloS one *7*, e52389.

Jicha, G. A., Bowser, R., Kazam, I. G., and Davies, P. (1997). Alz-50 and MC-1, a new monoclonal antibody raised to paired helical filaments, recognize conformational epitopes on recombinant tau. Journal of neuroscience research *48*, 128-132.

Kabeya, Y., Mizushima, N., Uero, T., Yamamoto, A., Kirisako, T., Noda, T., Kominami, E., Ohsumi, Y., and Yoshimori, T. (2000). LC3, a mammalian homologue of yeast Apg8p, is localized in autophagosome membranes after processing. Embo Journal *19*, 5720-5728.

Kam, T. I., Song, S., Gwon, Y., Park, H., Yan, J. J., Im, I., Choi, J. W., Choi, T. Y., Kim, J., Song, D. K., *et al.* (2013). FcgammaRIIb mediates amyloid-beta neurotoxicity and memory impairment in Alzheimer's disease. J Clin Invest *123*, 2791-2802.

Khurana, V., Elson-Schwab, I., Fulga, T. A., Sharp, K. A., Loewen, C. A., Mulkearns, E., Tyynela, J., Scherzer, C. R., and Feany, M. B. (2010). Lysosomal dysfunction promotes cleavage and neurotoxicity of tau in vivo. PLoS genetics *6*, e1001026.

Kim, M. Y., Ahn, K. Y., Lee, S. M., Koh, J. T., Chun, B. J., Bae, C. S., Lee, K. S., and Kim, K. K. (2004). The promoter of brain-specific angiogenesis inhibitor 1-associated protein 4 drives developmentally targeted transgene expression mainly in adult cerebral cortex and hippocampus. Febs Lett *566*, 87-94.

Kopeikina, K. J., Hyman, B. T., and Spires-Jones, T. L. (2012). Soluble forms of tau are toxic in Alzheimer's disease. Translational neuroscience *3*, 223-233.

Lasagna-Reeves, C. A., Castillo-Carranza, D. L., Sengupta, U., Clos, A. L., Jackson, G. R., and Kayed, R. (2011). Tau oligomers impair memory and induce synaptic and mitochondrial dysfunction in wild-type mice. Molecular neurodegeneration *6*, 39.

Lasagna-Reeves, C. A., Castillo-Carranza, D. L., Sengupta, U., Guerrero-Munoz, M.

J., Kiritoshi, T., Neugebauer, V., Jackson, G. R., and Kayed, R. (2012). Alzheimer brain-derived tau oligomers propagate pathology from endogenous tau. Scientific reports *2*, 700.

Lee, V. M., Goedert, M., and Trojanowski, J. Q. (2001). Neurodegenerative tauopathies. Annual review of neuroscience *24*, 1121-1159.

Lewis, J., McGowan, E., Rockwood, J., Melrose, H., Nacharaju, P., Van Slegtenhorst, M., Gwinn-Hardy, K., Paul Murphy, M., Baker, M., Yu, X., *et al.* (2000). Neurofibrillary tangles, amyotrophy and progressive motor disturbance in mice expressing mutant (P301L) tau protein. Nature genetics *25*, 402-405.

Lucas, J. J., Hernandez, F., Gomez-Ramos, P., Moran, M. A., Hen, R., and Avila, J. (2001). Decreased nuclear beta-catenin, tau hyperphosphorylation and neurodegeneration in GSK-3beta conditional transgenic mice. The EMBO journal *20*, 27-39.

Masliah, E., Terry, R. D., DeTeresa, R. M., and Hansen, L. A. (1989). Immunohistochemical quantification of the synapse-related protein synaptophysin in Alzheimer disease. Neuroscience letters *103*, 234-239.

Molinari, M., and Helenius, A. (1999). Glycoproteins form mixed disulphides with

oxidoreductases during folding in living cells. Nature *402*, 90-93.

Mondragon-Rodriguez, S., Mena, R., Binder, L. I., Smith, M. A., Perry, G., and Garcia-Sierra, F. (2008). Conformational changes and cleavage of tau in Pick bodies parallel the early processing of tau found in Alzheimer pathology. Neuropath Appl Neuro *34*, 62-75.

Newman, J., Rissman, R. A., Sarsoza, F., Kim, R. C., Dick, M., Bennett, D. A., Cotman, C. W., Rohn, T. T., and Head, E. (2005). Caspase-cleaved tau accumulation in neurodegenerative diseases associated with tau and alpha-synuclein pathology. Acta Neuropathol *110*, 135-144.

O'Leary, J. C., 3rd, Li, Q., Marinec, P., Blair, L. J., Congdon, E. E., Johnson, A. G., Jinwal, U. K., Koren, J., 3rd, Jones, J. R., Kraft, C.*, et al.* (2010). Phenothiazine-mediated rescue of cognition in tau transgenic mice requires neuroprotection and reduced soluble tau burden. Molecular neurodegeneration *5*, 45.

Oddo, S., Caccamo, A., Shepherd, J. D., Murphy, M. P., Golde, T. E., Kayed, R., Metherate, R., Mattson, M. P., Akbari, Y., and LaFerla, F. M. (2003). Triple-transgenic model of Alzheimer's disease with plaques and tangles: intracellular Abeta and synaptic dysfunction. Neuron *39*, 409-421.

Pankiv, S., Clausen, T. H., Lamark, T., Brech, A., Bruun, J. A., Outzen, H., Overvatn, A., Bjorkoy, G., and Johansen, T. (2007). p62/SQSTM1 binds directly to Atg8/LC3 to facilitate degradation of ubiquitinated protein aggregates by autophagy. Journal of Biological Chemistry *282*, 24131-24145.

Park, H., Kam, T. I., Kim, Y., Choi, H., Gwon, Y., Kim, C., Koh, J. Y., and Jung, Y. K. (2012). Neuropathogenic role of adenylate kinase-1 in Abeta-mediated tau phosphorylation via AMPK and GSK3beta. Human molecular genetics *21*, 2725-2737.

Patterson, K. R., Remmers, C., Fu, Y., Brooker, S., Kanaan, N. M., Vana, L., Ward, S., Reyes, J. F., Philibert, K., Glucksman, M. J., and Binder, L. I. (2011). Characterization of prefibrillar Tau oligomers in vitro and in Alzheimer disease. The Journal of biological chemistry *286*, 23063-23076.

Pickhardt, M., Gazova, Z., von Bergen, M., Khlistunova, I., Wang, Y., Hascher, A., Mandelkow, E. M., Biernat, J., and Mandelkow, E. (2005). Anthraquinones inhibit tau aggregation and dissolve Alzheimer's paired helical filaments in vitro and in cells. The Journal of biological chemistry *280*, 3628-3635.

Quintanilla, R. A., Matthews-Roberson, T. A., Dolan, P. J., and Johnson, G. V. (2009). Caspase-cleaved tau expression induces mitochondrial dysfunction in immortalized

cortical neurons: implications for the pathogenesis of Alzheimer disease. The Journal of biological chemistry *284*, 18754-18766.

Ravikumar, B., Vacher, C., Berger, Z., Davies, J. E., Luo, S., Oroz, L. G., Scaravilli, F., Easton, D. F., Duden, R., O'Kane, C. J., and Rubinsztein, D. C. (2004). Inhibition of mTOR induces autophagy and reduces toxicity of polyglutamine expansions in fly and mouse models of Huntington disease. Nature genetics *36*, 585-595.

Rissman, R. A., Poon, W. W., Blurton-Jones, M., Oddo, S., Torp, R., Vitek, M. P., LaFerla, F. M., Rohn, T. T., and Cotman, C. W. (2004). Caspase-cleavage of tau is an early event in Alzheimer disease tangle pathology. J Clin Invest *114*, 121-130.

Rohn, T. T., Rissman, R. A., Davis, M. C., Kim, Y. E., Cotman, C. W., and Head, E. (2002). Caspase-9 activation and caspase cleavage of tau in the Alzheimer's disease brain. Neurobiology of disease *11*, 341-354.

Sahara, N., Maeda, S., Murayama, M., Suzuki, T., Dohmae, N., Yen, S. H., and Takashima, A. (2007). Assembly of two distinct dimers and higher-order oligomers from full-length tau. The European journal of neuroscience *25*, 3020-3029.

Sanchez, I., Mahlke, C., and Yuan, J. (2003). Pivotal role of oligomerization in expanded polyglutamine neurodegenerative disorders. Nature *421*, 373-379.

Santacruz, K., Lewis, J., Spires, T., Paulson, J., Kotilinek, L., Ingelsson, M., Guimaraes, A., DeTure, M., Ramsden, M., McGowan, E., *et al.* (2005). Tau suppression in a neurodegenerative mouse model improves memory function. Science *309*, 476-481.

Schweers, O., Schonbrunn-Hanebeck, E., Marx, A., and Mandelkow, E. (1994). Structural studies of tau protein and Alzheimer paired helical filaments show no evidence for beta-structure. The Journal of biological chemistry *269*, 24290-24297.

Terwel, D., Lasrado, R., Snauwaert, J., Vandeweert, E., Van Haesendonck, C., Borghgraef, P., and Van Leuven, F. (2005). Changed conformation of mutant Tau-P301L underlies the moribund tauopathy, absent in progressive, nonlethal axonopathy of Tau-4R/2N transgenic mice. The Journal of biological chemistry *280*, 3963-3973.

Weaver, C. L., Espinoza, M., Kress, Y., and Davies, P. (2000). Conformational change as one of the earliest alterations of tau in Alzheimer's disease. Neurobiology of aging *21*, 719-727.

Wolfe, M. S. (2009). Tau mutations in neurodegenerative diseases. The Journal of biological chemistry *284*, 6021-6025.

Wood, N. I., Pallier, P. N., Wanderer, J., and Morton, A. J. (2007). Systemic administration of Congo red does not improve motor or cognitive function in R6/2 mice. Neurobiology of disease *25*, 342-353.

Zhang, Q. P., Zhang, X. G., and Sun, A. Y. (2009). Truncated tau at D421 is associated with neurodegeneration and tangle formation in the brain of Alzheimer transgenic models. Acta Neuropathol *117*, 687-697.

CHAPTER 2

Essential role of POLDIP2

in Tau aggregation and neurotoxicity via

autophagy/proteasome inhibition

Abstract

In Alzheimer's disease and other tauopathy, abnormal Tau proteins form intracellular aggregates and Tau filaments. However, the mechanisms that regulate Tau aggregation are not fully understood. In this paper, I show that POLDIP2 is a novel regulator of Tau aggregation. From a cell-based screening using cDNA expression library, I isolated POLDIP2 which increased Tau aggregation. Expression of POLDIP2 was increased in neuronal cells by the multiple stresses, including Aβ, TNF-α and H_2O_2. Accordingly, ectopic expression of POLDIP2 enhanced the formation of Tau aggregates without affecting Tau phosphorylation, while down-regulation of POLDIP2 alleviated ROS-induced Tau aggregation. Interestingly, I found that POLDIP2 overexpression induced impairments of autophagy activity and partially proteasome activity and this activities were retained in DUF525 domain of POLDIP2. In a drosophila model of human tauopathy, knockdown of the drosophila *POLDIP2* homolog, CG12162, attenuated rough eye phenotype induced by Tau overexpression. Further, the lifespan of neural-Tau^{R406W} transgenic files were recovered by CG12162 knockdown. Together, these observations indicate that POLDIP2 plays a crucial role in Tau

aggregation via the impairment of autophagy activity, providing insight into Tau aggregation in Tau pathology.

Introduction

Tau is a microtubule-associated protein that localizes mainly in the axon of neurons. Tau protein binds to and stabilizes microtubules and is highly soluble in normal condition (Schweers et al., 1994). On the contrary, Tau is hyperphosphorylated in AD and other tauopathies, during aging and under stress condition, leading to the formation of insoluble aggregates, known as neurofibrillary tangles (NFTs) in the affected neurons (Gotz et al., 1995). In familiar type AD, several genes that are involved in generating Aβ (*APP*, *PSEN1* and *PSEN2*) (Scheuner et al., 1996) or in frontotemporal dementia with parkinsonism 17, Tau itself (*TAU* P301L, R406W, V337M etc.) are closely related to onset of the disease (Hong et al., 1998). In most case (> 95%) of chronic AD and tauopathy, however, no single gene induces these diseases, and both age-related memory loss and increases rate of disease occurs with aging.

In general, the accumulation of Tau aggregates is critical for the pathogenesis in tauopathy. There seems to be a linkage between Tau aggregation and protein degradation machineries, the ubiquitin-proteasome system (UPS) and autophagy degradation pathway. UPS is the major

mechanism for protein quality control through selective degradation of damaged/unfolded proteins (Ciechanover, 2005). Autophagy also degrades cytosolic materials from proteins to organelles, especially insoluble protein aggregates (Cuervo, 2008). Accordingly, altered UPS function and autophagy degradation are frequently found in chronic neurodegenerative diseases, such as Alzheimer's disease (AD), Parkinson's disease (PD), Huntington's disease (HD) and amyotrophic lateral sclerosis (ALS) (Baehrecke, 2005; Ciechanover and Brundin, 2003). In these diseases, reduced activity of the degradation systems is accompanied by accumulation of the aggregation-prone proteins, such as Tau in tauopathy, including AD. However, cellular signal(s) and molecular determinant(s) responsible for the regulation of the degradation system and neuronal degeneration remain unknown.

Reactive oxygen species (ROS) often contributes to the development of neurodegenerative diseases (Barnham et al., 2004). Levels of ROSs are elevated during aging and increased in Alzheimer's disease (Christen, 2000). Mutant superoxide dismutase 1 (mSOD1) hetero knockout mice crossed with AD model mice show increased ROS and early impairment of learning/memory deficit (Bodendorf et al., 2002). Scavenging ROS suppresses neurotoxicity and reduces Tau aggregation, showing positive effects in animal models of neuronal diseases (Sung et al., 2004). Despite the

proposed contribution of ROS to neurodegeneration *in vitro* and *in vivo*, little is known about the molecular mechanism that ROS regulates the accumulation of aggregation-prone proteins underlying the neuropathology. POLDIP2 (also known as PDIP2, PDIP38) was first recognized as a protein that binds to DNA polymerase delta (Liu et al., 2003). POLDIP2 is predicted to interact with PCNA (Xie et al., 2005) and regulates NOX4 function in muscle cells (Lyle et al., 2009). However, the role of POLDIP2 in neurodegenerative disease is not understood.

In this paper, I identified POLDIP2 as an important modulator of Tau aggregation. I showed that POLDIP2 regulated Tau aggregation via the inhibition of autophagy and mediated neurotoxicity in a fly model expressing Tau.

Materials and methods

Cell culture and DNA transfection

Cell culture was previously described (Park et al., 2012). HEK293T, HeLa and SH-SY5Y cells were cultured in DMEM (Hyclone) supplemented with 10% (v/v) fetal bovine serum (Hyclone). Primary cortical neurons were prepared from mouse brains at embryonic day 16. The neurons were seeded on poly-L-lysine (0.01% in 100 mM borate buffer, pH 8.5)-coated plates and maintained in neurobasal medium containing 2% B-27 supplement (Invitrogen) and 0.5 mM L-glutamine. Half of the medium was exchanged every 3 days. HEK293T and SH-SY5Y cells were transfected using the Polyfect reagent (Qiagen).

Western blotting and antibodies

The lysates were prepared as described previously (Kam et al., 2013). The blots were blocked for 1 h and incubated with following antibodies: PHF-1, TG5 (a generous gift from Dr. P. Davies, Albert Einstein College of Medicine, USA), P3R and P8R (a gift from Dr. E. Klaile, Karolinska Institute, Sweden), FLAG (Sigma), α-tubulin, β-actin and GFP (Santa Cruz Biotechnology), p62,

ULK1, and p-ULK1 (Cell signaling) antibodies. Membranes were rinsed and incubated for 1 h with peroxidase-conjugated anti-mouse or rabbit antibody and visualized using the ECL detection system.

Filter trap assay for Tau aggregates

SH-SY5Y cells transfected with pcDNA3-HA and pPOLDIP2-HA with GFP-Tau cDNA and The lysates were prepared as described previously (Park et al., 2012). After brief sonication, equal amounts of cell lysates were passed through a nitrocellulose filter (0.2 mm). The membrane was washed three times with 1% SDS and blocked in the 5% non-fat milk for 1 h followed by immunoblotting.

DNA construction

To construct serial deletion mutants of human POLDIP2 (BC000655.2, polymerase delta-interacting protein 2 isoform 2), POLDIP2-WT (amino acids 1–368), POLDIP2-A (amino acids 201–368), POLDIP2-B (1–200), and POLDIP2-C (1–72) were amplified by PCR using gene-specific synthetic DNA oligonucleotides and subcloned into p3xFLAG-CMV-14.

Proteasome Activity Assays

Method for the assay is previously described (Shim et al., 2012). After preparation of cell lysates in lysis buffer, proteasome activities were measured using the fluorogenic substrates Suc-LLVY-AMC, Bz-VGR-AMC and Ac-GPLD-AMC (Biomol) and a fluorometer (FlexStation 3 Microplate Reader; Molecular Devices). The excitation and emission wavelengths were 380 and 460 nm, respectively.

Reverse transcription-PCR

Drosophila whole body were lyzed and total RNA was purified using Trizol reagent (Invitrogen) according to the manufacturer's protocol. PCR was performed using following synthetic oligonucleotides sets: CG12162 (5′-CCT CGA CCG CCT TTG AGA CGA ACG-3′, 5′- CGA GGT TCT CCA GTC GGA TGC AGT -3′), RP49 (5′- ATG ACC ATC CGC CCA GC-3′, 5′-CTC GTT CTC TTG AGA ACG-3′).

Small interfering RNA (siRNA) transfection

The siRNA oligonucleotides against POLDIP2 (#1, 1119184; #2, 1119188; #3, 1119189) and scrambled control were purchased (Bioneer) and RNA interference assay was done according to the manufacturer's instruction.

Transgenic Drosophila

D. melanogaster was raised in the dark at 25°C. WT (w^{1118}) and POLDIP2 mutant ($CG12162^{EY08866}$) strains used in this study were obtained from the Bloomington Drosophila Stock Center at Indiana University. The gl-$tau^{2.1}$ line was kindly provided by Dr. D. Geschwind (University of California, USA) (Jackson et al., 2002). UAS-tau^{R406W} fly line for the generation of elav-tau^{406W} was from Dr. M. Feany (Harvard Medical School, USA) (Wittmann et al., 2001).

Longevity assay

More than 200 files of each genotype were collected, divided into tubes of 10 flies and incubated at 29°C on the standard food. The culture medium was changed every 2 days and the numbers of dead files were recorded.

Results

Identification of POLDIP2 as an inducer of Tau aggregation

To find out new regulator(s) of Tau protein aggregation, I screened 5,000 cDNAs encoding protein kinases, membrane proteins and other proteins that are expressed in the brain and are associated with human diseases (Shim et al., 2012). With the cell-based assay using GFP-Tau, GFP allowed the detection and formation of Tau aggregates under a fluorescence microscope. During the screening, transfection efficiency was normalized by cotransfection with monomeric RFP. GFP-positive dots were counted as aggregates of the Tau. From screening using the expression library, I could isolate putative positive cDNA clones (Fig. 2-1A and B). Ectopic expression of the putative positive clones enhanced the aggregation of GFP-Tau in the transfected cells (Fig. 2-1B). In particular, POLDIP2 overexpression exhibited strong effects on the aggregation of GFP-Tau (Fig. 2-1C) and induced neuronal cell death (Fig. 2-1D) in a dose-dependent manner.

The expression of POLDIP2 is increased by reactive oxygen stress for Tau aggregation

Then I investigated the signal that might regulate the expression of POLDIP2. Interestingly, I found that treatment with amyloid beta$_{1-42}$ (Aβ), a pathogenic factor of AD (Kam et al., 2013), tumor necrosis factor alpha (TNF-α) or H_2O_2 increased the expression of POLDIP2 in mouse primary hippocampal neurons, while other signals did not affect it (Fig. 2-2A). All these signals are believed to be crucial in many neurodegenerative disease (Schwab and McGeer, 2008). Among these signals, I focused on ROS because this signal is highly associated with sporadic type of neurodegenerative disease but its mechanism is not known yet (Glass et al., 2010). Treatment with H_2O_2 also increased POLDIP2 expression in SH-SY5Y human neuroblastoma cells (Fig. 2-2B).

Next, I addressed whether ROS could affect Tau aggregation. The results from cell-based GFP-Tau dot formation assay showed that treatment with H_2O_2 increased the numbers of GFP-Tau aggregates in SH-SY5Y cells (Fig. 2-3A). In addition, H_2O_2 increased the amounts of detergent-insoluble tau aggregates on filter-trap assay (Fig. 2-3B). With the notion that POLDIP2 expression was induced by ROS, I examined whether POLDIP2 was involved with the aggregation of Tau. I found that POLDIP2 expression was significantly reduced by POLDIP2 siRNA#1 and 2, and marginally by POLDIP2 siRNA#3 (Fig. 2-3C). Interestingly, knockdown of POLDIP2

expression by POLDIP2 siRNA#1 or 2, but not POLDIP2 siRNA#3, inhibited ROS-induced Tau aggregates (Fig. 2-3D). These results indicate that POLDIP2 is critical in Tau aggregation induced by ROS.

Increased POLDIP2 impairs autophagy activity

Many studies have shown that the aggregation of Tau protein is accompanied by Tau hyperphosphorylation, a typical pathophysiologic modification of Tau (Park et al., 2012). When I examined Tau phosphorylation with western blot analysis, however, ROS or overexpression of POLDIP2 did not much affect the phosphorylation status of Tau protein (Fig. 2-3B). These results led us to address a possibility that POLDIP2 might interfere the clearance of Tau protein by affecting autophagy and UPS. In addition, it was shown that multiple stresses, including ROS and Aβ, impair the activity of affect autophagy flux (Scherz-Shouval and Elazar, 2011) and proteasome complex (Aiken et al., 2011). Especially, aggregation-prone proteins, including Tau aggregates, are believed to be clarified by autophagy (Wang et al., 2009).

Thus, I examined whether POLDIP2 affected autophagy activity using mCherry-GFP-LC3. In the mCherry-GFP-LC3 assay, inhibition of lysosomal activity displays $mCherry^{+}/GFP^{+}$ double-positive puncta because of the

localization of acid-labile GFP-LC3 in autolysosomes, while acid-sensitive GFP signals normally disappear in autolysosomes. Interestingly, I found that overexpression of POLDIP2 drastically increased the formation of colocalized mCherry-GFP dots and reduced the numbers of mCherry-only cells (Fig. 2-4A), indicating an inhibition in late autolysosome function (Pankiv et al., 2007). Accordingly, I found that overexpressed POLDIP2 greatly increased the levels of LC3 II and p62 (Fig. 2-4B), an ubiquitin-binding autophagy receptor (Lamark et al., 2009). Consistent to the recent report (Brown et al., 2014), knockdown of POLDIP2 expression enhanced autophagy activity (Fig. 2-4C). These results strongly suggest that increased POLDIP2 impairs autophagy. I further assessed proteasome activity and found that ROS inhibited enzymatic activity of proteasome in SH-SY5Y cells (Fig. 2-5A). Knockdown of POLDIP2 expression partially but not much rescued the impairment of proteasome activity by ROS (Fig. 2-5B). In addition, ectopic expression of POLDIP2 marginally increased the accumulation of unstable degron (Fig. 2-5C) and suppressed proteasome activity (Fig. 2-5D).

The POLDIP2 regulates Tau aggregation and autophagy via DUF525 domain

The POLDIP2 has 2 distinct domains; Yccv-like domain and DUF525 domain (Brown et al., 2014). To define the domain(s) responsible for Tau aggregation, several deletion mutants of POLDIP2 were generated (Fig. 2-6A). From western blot analysis, I observed similar levels of expression among POLDIP2 full-length and two deletion mutants except POLDIP2-C mutant which was not expressed in the transfected cells (Fig. 2-6B). Like POLDIP2, POLDIP2-A mutant containing the DUF525 domain only effectively increased Tau aggregation, while POLDIP2-B mutant containing the Yccv-like domain and POLDIP2-C mutant lacking both Yccv-like domain and DUF525 domain did not stimulate Tau aggregation (Fig. 2-6C).

Interestingly, I found that POLDIP2-A containing the DUF525 domain only, but not POLDIP2-B mutant, increased colocalization of mCherry and GFP dots and reduced the numbers of mCherry-only cells as much as POLDIP2 did (Fig. 2-6D). These results indicate that the DUF525 domain is crucial for autophagy inhibitory function of POLDIP2 and suggest a strong correlation between Tau aggregation and autophagy inhibition exhibited by POLDIP2. Unlike their effects on autophagy inhibition, I could not find any clear correlation between Tau aggregation by the POLDIP2 mutants and their effects on proteasome inhibition (Fig. 2-7).

POLDIP2 knockout rescues human Tau-mediated neural degeneration in drosophila

To assess an *in vivo* role of POLDIP2 in Tau pathology, I used a drosophila model expressing Tau in the eye (Jackson et al., 2002) and whole-neurons (Wittmann et al., 2001). The flies with the retinal overexpression of human Tau (gl-tau$^{2.1}$) showed moderate toxicity, characterized by the loss of photoreceptor neurons, leading to observation in drosophila eye as a rough surface (Fig. 2-8A). The *CG12162* gene has been identified as a fly homolog of the POLDIP2 and 1 p-element insertion mutant line (Bloomington stock No.17500, CG12162^{EY08866}) showed reduced level of *CG12162* mRNA (Fig. 2-9A). Then I reconstituted the knockout flies (CG12162$^{\Delta EY08866}$) by ejecting p-element from CG12162^{EY08866} flies. Compared with that in control flies (w^{1118}), there was no detectible difference in the eye morphology of *CG12162* knockout flies or CG12162$^{\Delta EY08866}$ reconstituted flies (Fig. 2-8A, left 3 panels).

Then I crossed CG12162^{EY08866} mutant or CG12162$^{\Delta EY08866}$ reconstitution flies with gl-tau$^{2.1}$ Tau flies. Interestingly, knockdown of fly POLDIP2 homologue in the retina of Tau transgenic flies (gl-tau$^{2.1}$/CG12162^{EY08866}) markedly rescued Tau-induced retinal degeneration. On the contrary, reconstitution of CG12162^{EY08866} fly in Tau flies (gl-tau$^{2.1}$/CG12162$^{\Delta EY08866}$)

again caused rough eye phenotype (Fig. 2-8A, right 3 panels). These observations indicate that POLDIP2 level is critical in Tau-induced neurotoxicity in the flies. Compared with Tau transgenic flies, the results from western blot analysis revealed that Tau phosphorylation at PHF-1 epitope (Ser 396/404) was not affected by knockdown of fly POLDIP2 homologue in the fly eye expressing Tau (gl-tau$^{2.1}$/CG12162^{EY08866}) (Fig. 2-9B), consistent to those of our cell models. Similarly, other Drosophila tau model also showed that ROS exacerbates tau toxicity without altering tau phosphorylation (Dias-Santagata et al., 2007).

Further, I crossed wild-type, CG12162 mutant or CG12162 reconstitution flies with Tau^{R406W} flies which express Tau^{R406W} in whole neurons (Wittmann et al., 2001), and compared their lifespan. Tau flies (elav-gal4;UAS-Tau^{R406W}) exhibited shorter lifespan (average 35 days) than control flies (elav-gal4/+, average 45 days). When Tau flies were crossed with POLDIP2 mutant flies (CG12162^{EY08866}) or reconstituted flies (CG12162$^{\Delta EY08866}$), the lifespan was significantly extended by POLDIP2 deficiency (average 42 days in elav-gal4; UAS-Tau^{R406W}/CG12162^{EY08866}) but not in the reconstituted line (average 35 days in elav-gal4; UAS-Tau^{R406W}/CG12162$^{\Delta EY08866}$) (Fig. 2-8B). Thus, these observations further support that POLDIP2 plays an important role in Tau-mediated neurodegeneration in a model organism.

Figure 2-1. Isolation of POLDIP2 as a regulator of Tau aggregation. (A) The 5,000 cDNAs in mammalian expression vector were screened by a cell-based assay using GFP-Tau, as shown in scheme. (B) SH-SY5Y cells were transfected with GFP-Tau alone or together with GSK3β or putative positive clones for 24 h. Cells showing Tau aggregates were counted under fluorescence microscope. (C) SH-SY5Ycells were transfected with GFP-Tau and the increasing amounts of POLDIP2 for 24 h and GFP-Tau aggregation was then analyzed under microscope. (D) SH-SY5Ycells were transfected with POLDIP2 for 24 h and cell death was analyzed. Data are means ± S.D. ($p < 0.05$).

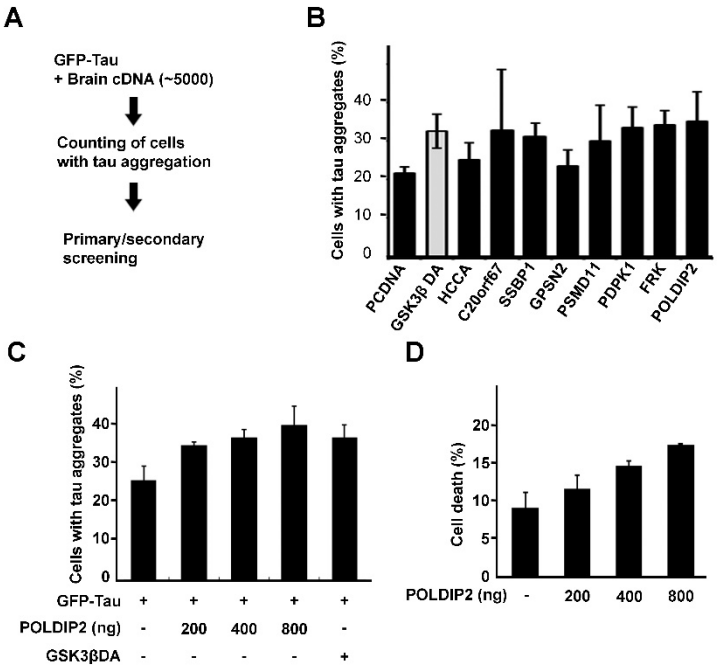
A
GFP-Tau
+ Brain cDNA (~5000)
Counting of cells
with tau aggregation
Primary/secondary
screening
B
Cells with tau aggregates (%)
0
10
20
30
40
PCDNA
GSK3β DA
HCCA
C20orf67
SSBP1
GPSN2
PSMD11
PDPK1
FRK
POLDIP2
C
Cells with tau aggregates (%)
0
10
20
30
40
GFP-Tau + + + + +
POLDIP2 (ng) - 200 400 800 -
GSK3βDA - - - - +
D
Cell death (%)
0
5
10
15
20
POLDIP2 (ng) - 200 400 800

Figure 2-2. POLDIP2 expression is increased by oxidative stress in SH-SY5Y cells and cultured primary neurons.

(A) Primary cortical neurons were treated with 50 ng/ml TNF-α, 200 μM H_2O_2 or 5 μM $A\beta_{1-42}$ and then analyzed by western blotting. (B) SH-SY5Y cells were incubated with the increasing doses of H_2O_2 for 24 h and analyzed by western blotting.

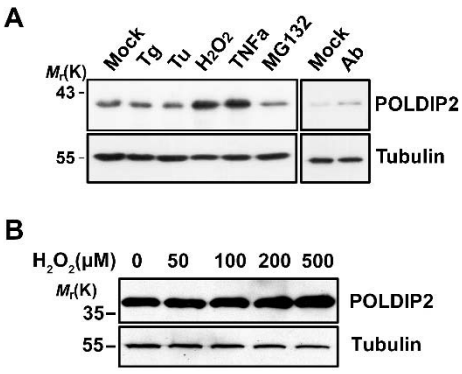
A
Mock
Tg
Tu
H2O2
TNFa
MG132
Mock
Ab
Mr(K)
43
55
POLDIP2
Tubulin
B
H2O2(μM) 0 50 100 200 500
Mr(K)
35
55
POLDIP2
Tubulin

Figure 2-3. Knockdown of POLDIP2 expression inhibits oxidative stress-induced Tau aggregation.

(A) SH-SY5Y cells were transfected with GFP-Tau and then incubated with 200 μM H_2O_2 for 24 h. Tau aggregates were then observed under fluorescence microscope. (B) Samples from (A) were analyzed by filter-trap assay and Western blot. (C) SH-SY5Y cells were transfected with POLDIP siRNA (#1, 2, and 3). After 48 h, cells were analyzed for POLDIP2 knockdown by western blotting. (D) SH-SY5Y cells were cotransfected with POLDIP siRNA and GFP-Tau. After 48 h, Tau aggregation were analyzed under fluorescence microscope. Data are means ± S.D. ($n > 3$).

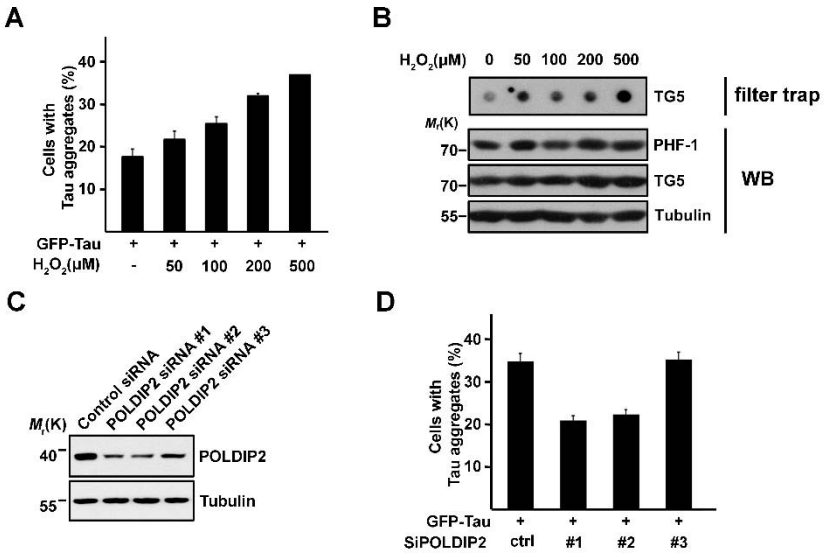
A
Cells with Tau aggregates (%)
40
30
20
10
GFP-Tau + + + + +
H2O2(μM) - 50 100 200 500
B
H2O2(μM) 0 50 100 200 500
TG5
filter trap
Mr(K)
70
PHF-1
70
TG5
WB
55
Tubulin
C
Mr(K)
Control siRNA
POLDIP2 siRNA #1
POLDIP2 siRNA #2
POLDIP2 siRNA #3
40
POLDIP2
55
Tubulin
D
Cells with Tau aggregates (%)
40
30
20
10
GFP-Tau + + + +
SiPOLDIP2 ctrl #1 #2 #3

Figure 2-4. POLDIP2 expression impairs autophagy flux.

(A) HeLa cells were cotransfected with POLDIP2 and GFP-mCherry-LC3 for 24 h. Numbers of RFP only-positive or GFP/RFP-colocalized cells were counted and represented as bar graph. (B) SH-SY5Ycells were transfected with POLDIP2 and cell lysates were analyzed with western blotting. (C) SH-SY5Y cells were cotransfected with GFP-LC3 and POLDIP2 siRNA (#1, 2, and 3) and GFP-LC3 dot formation was counted under fluorescence microscope. Data are means ± S.D. ($n > 3$).

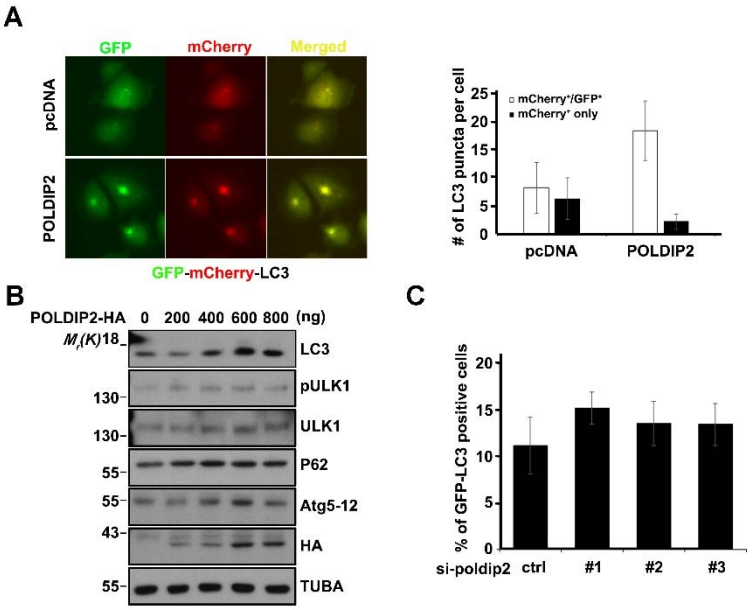
A
GFP
mCherry
Merged
pcDNA
POLDIP2
GFP-mCherry-LC3
mCherry+/GFP+
mCherry+ only
# of LC3 puncta per cell
pcDNA
POLDIP2
B
POLDIP2-HA 0 200 400 600 800 (ng)
Mr(K)
18
LC3
130
pULK1
130
ULK1
55
P62
55
Atg5-12
43
HA
55
TUBA
C
% of GFP-LC3 positive cells
si-poldip2 ctrl #1 #2 #3

Figure 2-5. **Increased POLDIP2 impairs proteasome activity.**

SH-SY5Y cells were incubated with 200μM H_2O_2 for 24 h and chymotrypsin-like proteasome activity was measured using Suc-LLVY-AMC (A). SH-SY5Y cells were transfected with POLDIP2 siRNA (#1, 2 or 3). After 48 h, cells were treated with 200μM H_2O_2 for additional 24 h and analyzed for proteasome activity (B). SH-SY5Y cells were cotransfected POLDIP2 with green fluorescent protein tagged with CL1 (GFP^u) for 36 h and then analyzed by western blotting (left) and the signals on the blot were quantified by densitometric analysis (right) (C). SH-SY5Y cells were transfected with POLDIP2 (400 and 800 ng/ml) for 24 h and chymotrypsin-like activity was then measured using Suc-LLVY-AMC (D). Data are means ± S.D. ($n > 3$).

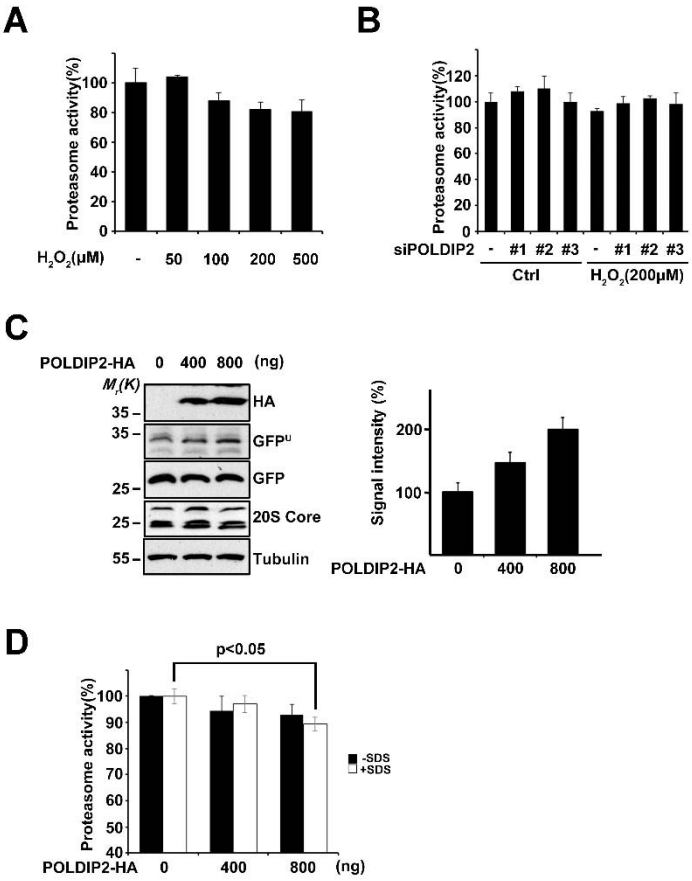
A
Proteasome activity(%)
100
80
60
40
20
0
H2O2(μM) - 50 100 200 500
B
Proteasome activity(%)
120
100
80
60
40
20
0
siPOLDIP2 - #1 #2 #3 - #1 #2 #3
Ctrl
H2O2(200μM)
C
POLDIP2-HA 0 400 800 (ng)
MA(K)
35
35
25
25
55
HA
GFPu
GFP
20S Core
Tubulin
Signal intensity (%)
200
100
POLDIP2-HA 0 400 800
D
p<0.05
Proteasome activity(%)
100
90
80
70
60
50
40
-SDS
+SDS
POLDIP2-HA 0 400 800 (ng)

Figure 2-6. **POLDIP2 regulates Tau aggregation and autophagy flux through its DUF525 domain**.

(A) Schematic diagram of POLDIP2 domains and its deletion mutants. Numbers indicate amino-acid residues of human POLDIP2. (B) Western blot analysis showing expression of the transfected POLDIP2 wild-type (WT) and 3 deletion mutants in HEK293T cells. (C-D) SH-SY5Y cells were cotransfected with POLDIP2 deletion mutants and GFP-Tau (C) or GFP-mCherry-LC3 (D). After 24 h, Tau aggregation (C) and LC3 puncta formation (D) were examined under microscope. The effects of POLDIP2 mutants on Tau aggregation and autophagy activity are summarized in (A). Data are means ± S.D. ($n > 3$).

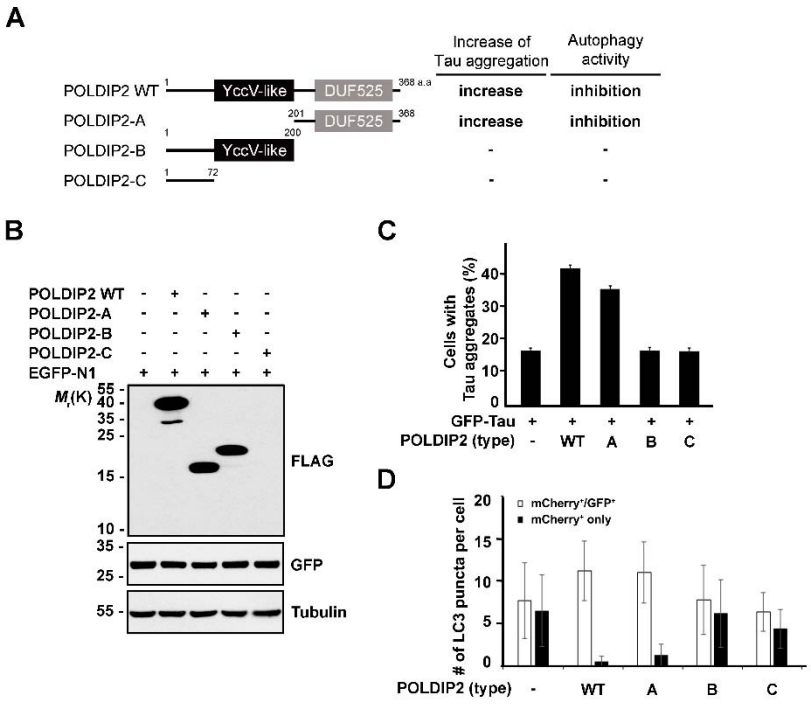
A
Increase of Tau aggregation
Autophagy activity
POLDIP2 WT
YccV-like
DUF525
368 a.a
increase
inhibition
POLDIP2-A
DUF525
increase
inhibition
POLDIP2-B
YccV-like
POLDIP2-C
B
POLDIP2 WT
POLDIP2-A
POLDIP2-B
POLDIP2-C
EGFP-N1
Mr(K)
FLAG
GFP
Tubulin
C
Cells with Tau aggregates (%)
GFP-Tau
POLDIP2 (type)
WT
A
B
C
D
mCherry+/GFP+
mCherry+ only
# of LC3 puncta per cell
POLDIP2 (type)

Figure 2-7. **POLDIP2 does not affect proteasome activity.**

(A) SH-SY5Y cells were transfected with POLDIP2 deletion mutants. After 24 h, proteasome activity were measured using GFP^{U} accumulation. (B) Cell lysates from (A) were analyzed for proteasome activity using the fluorogenic substrate Suc-LLVY-AMC with fluorometer.

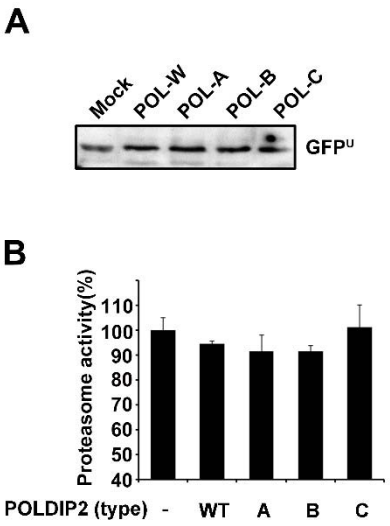
A
Mock
POL-W
POL-A
POL-B
POL-C
GFPU
B
Proteasome activity(%)
110
100
90
80
70
60
50
40
POLDIP2 (type) -
WT
A
B
C

Figure 2-8. **Knockdown of POLDIP2 expression rescues Tau toxicity in a Drosophila model.**

(A) WT (w^{1118}) and POLDIP2 knockdown mutant ($CG12162^{EY08866}$), and POLDIP2-reconstituted ($CG12162^{\Delta EY08866}$) flies were crossed with flies showing tau rough eye (gl-$tau^{2.1}$), generating double transgenic fly lines (gl-$tau^{2.1}$/$CG12162^{EY08866}$ and gl-$tau^{2.1}$/$CG12162^{\Delta EY08866}$). Eye morphology of each line was examined. (B) Flies expressing Tau^{R406W} in whole body neurons (elav-gal4; UAS-Tau^{R406W}) were crossed with POLDIP2 knockdown mutant flies, generating double transgenic flies (elav-gal4; UAS-Tau^{R406W}/$CG12162^{EY08866}$) and with POLDIP2-reconstituted flies, generating double transgenic flies (elav-gal4; UAS-Tau^{R406W}/$CG12162^{\Delta EY08866}$). Flies were collected at 1 day after eclosion and lifespan was measured at 29°C (n > 200).

A


gmr-GAL4
CG12162EY08866
CG12162ΔEY08866
gl-Tau2.1
gl-Tau2.1 /CG12162EY08866
gl-Tau2.1 /CG12162ΔEY08866

B

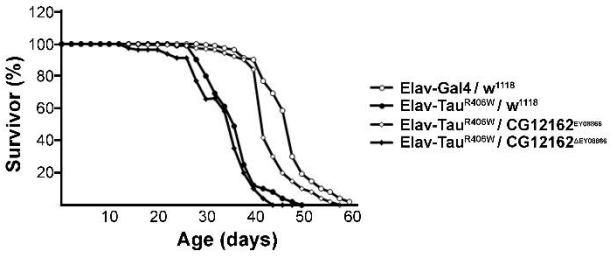
Survivor (%)
120
100
80
60
40
20
10
20
30
40
50
60
Age (days)
Elav-Gal4 / w1118
Elav-TauR406W / w1118
Elav-TauR406W / CG12162EY08866
Elav-TauR406W / CG12162ΔEY08866

Figure 2-9. **Deficiency of *Drosophila* POLDIP2 homologue in flies does not alter Tau phosphorylation.**

(A) Total RNA was purified from wild-type (w^{1118}) and POLDIP2 knockdown mutant (CG12162^{EY08866}) and analyzed with RT-PCR. (B) WT (w^{1118}) and POLDIP2 mutant (CG12162^{EY08866}), and POLDIP2-reconstituted (CG12162$^{\Delta EY08866}$) flies were crossed with the flies showing tau rough eye (gl-tau$^{2.1}$) and fly head extracts were analyzed by Western blotting.

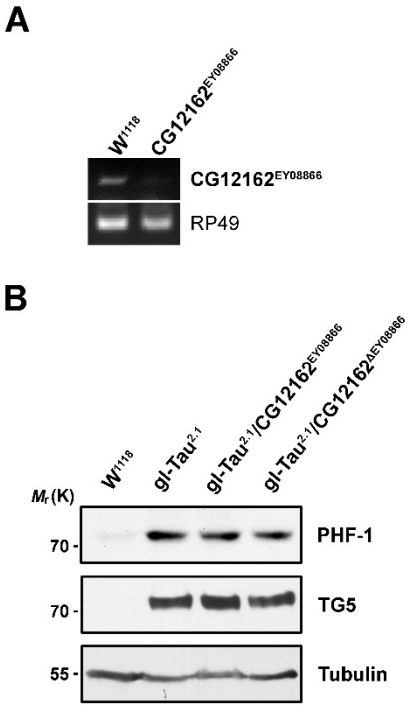
A
W1118
CG12162EY08866
CG12162EY08866
RP49
B
W1118
gl-Tau2-1
gl-Tau2-1/CG12162EY08866
gl-Tau2-1/CG12162ΔEY08866
Mr (K)
70
PHF-1
70
TG5
55
Tubulin

DISCUSSION

Despite the discrepancy between Tau protein aggregation and neurodegeneration, NFTs are considered as a major pathogenic factor in tauopathy. Intracellular accumulation of Tau and neurofibrillary degeneration are hallmark of tauopathies, including AD. In this study employing genome-wide screening and subsequent characterization, I found that POLDIP2 is an important player in Tau aggregation and Tau-associated neuropathology. Unlike other pathogenic mediators, such as GSK3β and Cdk5 (Yamaguchi et al., 1996), in Tau aggregation, POLDIP2 does not alter Tau phosphorylation but regulates Tau degradation/clearance system. Especially, it is interesting to note that the POLDIP2 regulates autophagy flux through DUF525 domain which consists of two subdomains, ApaG and F-box c-terminal like subdomain and is predicted to be involved in protein-protein interactions (Winston et al., 1999).

Though POLDIP2 was reported as a polymerase delta interaction protein (Liu et al., 2003), it seems to be a multifunctional protein. POLDIP2 is also known as a regulator of NOX4; in smooth muscle cells, POLDIP2 induces RhoA via NOX4 activation (Lyle et al., 2009) and RhoA – ROCK

(Rho kinase) increases Tau-mediated neurodegeneration and RhoA and Rock inhibition by Rock inhibitor reduces Tau protein level (Hamano et al., 2012). Also, RhoA and Rock inhibition stimulates protein degradation system (Bauer et al., 2009). Thus, POLDIP2 might form a positive feedback loop under ROS stimulation and inhibits protein degradation pathways. Although the previous studies showed that autophagy is upregulated in POLDIP2 knockout mouse embryo fibroblasts (Brown et al., 2014), the mechanism by which POLDIP2 regulates autophagy remains to be addressed.

Autophagy and proteasome activities are declined during aging, while ROS are increased. Thus, dysregulation of these factors affects longevity and accelerates aging (Min et al., 2008; Rubinsztein et al., 2011). In addition to its effect on aging, global autophagy impairment also causes the aggregation of misfolded proteins, which is associated with perturbation of cellular functions and various human disorders. Moreover, ROS is an important pathophysiological feature of many neurodegenerative diseases and exacerbates the progression of neurodegenerative diseases (Nixon, 2013). Consistently, neurodegenerative model mice with SOD mutation show neurodegeneration with multiple protein aggregation (Bodendorf et al., 2002). Most studies, however, have focused on the degradation systems of the oxidized proteins or ROS-damaged organelles, such as mitochondria (Scherz-

Shouval and Elazar, 2007). On the other hand, our study illustrates an important mediator, POLDIP2, of ROS to impair autophagy pathway. Thus, enhancement of autophagy activity by the inhibition of POLDIP2 may provide an insight into manipulation of Tau-associated neuronal degeneration, as evidenced by the Tau fly model with POLDIP2 deficiency.

In conclusion, I propose that POLDIP2 plays an important role in a tauopathy model through the regulation of autophagy activity, linking the ROS signal to neuronal degeneration possibly in sporadic neurodegenerative diseases.

REFERENCES

Aiken, C. T., Kaake, R. M., Wang, X., and Huang, L. (2011). Oxidative stress-mediated regulation of proteasome complexes. Molecular & cellular proteomics : MCP *10*, R110.006924.

Baehrecke, E. H. (2005). Autophagy: dual roles in life and death? Nature reviews Molecular cell biology *6*, 505-510.

Barnham, K. J., Masters, C. L., and Bush, A. I. (2004). Neurodegenerative diseases and oxidative stress. Nature reviews Drug discovery *3*, 205-214.

Bauer, P. O., Wong, H. K., Oyama, F., Goswami, A., Okuno, M., Kino, Y., Miyazaki, H., and Nukina, N. (2009). Inhibition of Rho kinases enhances the degradation of mutant huntingtin. The Journal of biological chemistry *284*, 13153-13164.

Bodendorf, U., Danner, S., Fischer, F., Stefani, M., Sturchler-Pierrat, C., Wiederhold, K. H., Staufenbiel, M., and Paganetti, P. (2002). Expression of human beta-secretase in the mouse brain increases the steady-state level of beta-amyloid. Journal of neurochemistry *80*, 799-806.

Brown, D. I., Lassegue, B., Lee, M., Zafari, R., Long, J. S., Saavedra, H. I., and

Griendling, K. K. (2014). Poldip2 knockout results in perinatal lethality, reduced cellular growth and increased autophagy of mouse embryonic fibroblasts. PloS one *9*, e96657.

Christen, Y. (2000). Oxidative stress and Alzheimer disease. The American journal of clinical nutrition *71*, 621s-629s.

Ciechanover, A. (2005). Intracellular protein degradation: from a vague idea thru the lysosome and the ubiquitin-proteasome system and onto human diseases and drug targeting. Cell death and differentiation *12*, 1178-1190.

Ciechanover, A., and Brundin, P. (2003). The ubiquitin proteasome system in neurodegenerative diseases: sometimes the chicken, sometimes the egg. Neuron *40*, 427-446.

Cuervo, A. M. (2008). Autophagy and aging: keeping that old broom working. Trends in genetics : TIG *24*, 604-612.

Dias-Santagata, D., Fulga, T. A., Duttaroy, A., and Feany, M. B. (2007). Oxidative stress mediates tau-induced neurodegeneration in Drosophila. J Clin Invest *117*, 236-245.

Glass, C. K., Saijo, K., Winner, B., Marchetto, M. C., and Gage, F. H. (2010).

Mechanisms underlying inflammation in neurodegeneration. Cell *140*, 918-934.

Gotz, J., Probst, A., Spillantini, M. G., Schafer, T., Jakes, R., Burki, K., and Goedert, M. (1995). Somatodendritic localization and hyperphosphorylation of tau protein in transgenic mice expressing the longest human brain tau isoform. The EMBO journal *14*, 1304-1313.

Hamano, T., Yen, S. H., Gendron, T., Ko, L. W., and Kuriyama, M. (2012). Pitavastatin decreases tau levels via the inactivation of Rho/ROCK. Neurobiology of aging *33*, 2306-2320.

Hong, M., Zhukareva, V., Vogelsberg-Ragaglia, V., Wszolek, Z., Reed, L., Miller, B. I., Geschwind, D. H., Bird, T. D., McKeel, D., Goate, A., *et al.* (1998). Mutation-specific functional impairments in distinct tau isoforms of hereditary FTDP-17. Science *282*, 1914-1917.

Jackson, G. R., Wiedau-Pazos, M., Sang, T. K., Wagle, N., Brown, C. A., Massachi, S., and Geschwind, D. H. (2002). Human wild-type tau interacts with wingless pathway components and produces neurofibrillary pathology in Drosophila. Neuron *34*, 509-519.

Kam, T. I., Song, S., Gwon, Y., Park, H., Yan, J. J., Im, I., Choi, J. W., Choi, T. Y.,

Kim, J., Song, D. K., *et al.* (2013). FcgammaRIIb mediates amyloid-beta neurotoxicity and memory impairment in Alzheimer's disease. J Clin Invest *123*, 2791-2802.

Lamark, T., Kirkin, V., Dikic, I., and Johansen, T. (2009). NBR1 and p62 as cargo receptors for selective autophagy of ubiquitinated targets. Cell cycle (Georgetown, Tex) *8*, 1986-1990.

Liu, L., Rodriguez-Belmonte, E. M., Mazloum, N., Xie, B., and Lee, M. Y. (2003). Identification of a novel protein, PDIP38, that interacts with the p50 subunit of DNA polymerase delta and proliferating cell nuclear antigen. The Journal of biological chemistry *278*, 10041-10047.

Lyle, A. N., Deshpande, N. N., Taniyama, Y., Seidel-Rogol, B., Pounkova, L., Du, P., Papaharalambus, C., Lassegue, B., and Griendling, K. K. (2009). Poldip2, a novel regulator of Nox4 and cytoskeletal integrity in vascular smooth muscle cells. Circulation research *105*, 249-259.

Min, J. N., Whaley, R. A., Sharpless, N. E., Lockyer, P., Portbury, A. L., and Patterson, C. (2008). CHIP deficiency decreases longevity, with accelerated aging phenotypes accompanied by altered protein quality control. Molecular and cellular biology *28*, 4018-4025.

Nixon, R. A. (2013). The role of autophagy in neurodegenerative disease. Nature medicine *19*, 983-997.

Pankiv, S., Clausen, T. H., Lamark, T., Brech, A., Bruun, J. A., Outzen, H., Overvatn, A., Bjorkoy, G., and Johansen, T. (2007). p62/SQSTM1 binds directly to Atg8/LC3 to facilitate degradation of ubiquitinated protein aggregates by autophagy. Journal of Biological Chemistry *282*, 24131-24145.

Park, H., Kam, T. I., Kim, Y., Choi, H., Gwon, Y., Kim, C., Koh, J. Y., and Jung, Y. K. (2012). Neuropathogenic role of adenylate kinase-1 in Abeta-mediated tau phosphorylation via AMPK and GSK3beta. Human molecular genetics *21*, 2725-2737.

Rubinsztein, D. C., Marino, G., and Kroemer, G. (2011). Autophagy and aging. Cell *146*, 682-695.

Scherz-Shouval, R., and Elazar, Z. (2007). ROS, mitochondria and the regulation of autophagy. Trends in cell biology *17*, 422-427.

Scherz-Shouval, R., and Elazar, Z. (2011). Regulation of autophagy by ROS: physiology and pathology. Trends in biochemical sciences *36*, 30-38.

Scheuner, D., Eckman, C., Jensen, M., Song, X., Citron, M., Suzuki, N., Bird, T. D., Hardy, J., Hutton, M., Kukull, W., *et al.* (1996). Secreted amyloid beta-protein similar to that in the senile plaques of Alzheimer's disease is increased in vivo by the presenilin 1 and 2 and APP mutations linked to familial Alzheimer's disease. Nature medicine *2*, 864-870.

Schwab, C., and McGeer, P. L. (2008). Inflammatory aspects of Alzheimer disease and other neurodegenerative disorders. Journal of Alzheimer's disease : JAD *13*, 359-369.

Schweers, O., Schonbrunn-Hanebeck, E., Marx, A., and Mandelkow, E. (1994). Structural studies of tau protein and Alzheimer paired helical filaments show no evidence for beta-structure. The Journal of biological chemistry *269*, 24290-24297.

Shim, S. M., Lee, W. J., Kim, Y., Chang, J. W., Song, S., and Jung, Y. K. (2012). Role of S5b/PSMD5 in proteasome inhibition caused by TNF-alpha/NFkappaB in higher eukaryotes. Cell reports *2*, 603-615.

Sung, S., Yao, Y., Uryu, K., Yang, H., Lee, V. M., Trojanowski, J. Q., and Pratico, D. (2004). Early vitamin E supplementation in young but not aged mice reduces Abeta levels and amyloid deposition in a transgenic model of Alzheimer's disease. FASEB journal : official publication of the Federation of American Societies for

Experimental Biology *18*, 323-325.

Wang, Y., Martinez-Vicente, M., Kruger, U., Kaushik, S., Wong, E., Mandelkow, E. M., Cuervo, A. M., and Mandelkow, E. (2009). Tau fragmentation, aggregation and clearance: the dual role of lysosomal processing. Human molecular genetics *18*, 4153-4170.

Winston, J. T., Koepp, D. M., Zhu, C., Elledge, S. J., and Harper, J. W. (1999). A family of mammalian F-box proteins. Curr Biol *9*, 1180-1182.

Wittmann, C. W., Wszolek, M. F., Shulman, J. M., Salvaterra, P. M., Lewis, J., Hutton, M., and Feany, M. B. (2001). Tauopathy in Drosophila: neurodegeneration without neurofibrillary tangles. Science *293*, 711-714.

Xie, B., Li, H., Wang, Q., Xie, S., Rahmeh, A., Dai, W., and Lee, M. Y. (2005). Further characterization of human DNA polymerase delta interacting protein 38. The Journal of biological chemistry *280*, 22375-22384.

Yamaguchi, H., Ishiguro, K., Uchida, T., Takashima, A., Lemere, C. A., and Imahori, K. (1996). Preferential labeling of Alzheimer neurofibrillary tangles with antisera for tau protein kinase (TPK) I/glycogen synthase kinase-3 beta and cyclin-dependent kinase 5, a component of TPK II. Acta neuropathologica *92*, 232-241.

국문 초록

알츠하이머 병(alzheimer's disease)과 다른 tau에 의한 퇴행성 뇌질환에서 tau 단백질은 세포내 응집현상(aggregated) 과 filament를 형성한다. 이러한 tau의 중합체(oligomer)들은 이러한 퇴행성질환에서 신경독성을 일으키는 가장 큰 원인 중 하나로 알려져 있다. 그러나 이러한 Tau단백질의 aggregation의 형성과 조절에 관련된 기작이나 유전자에 대해서 아직 밝혀지지 않은 부분이 많다. 이 논문에서는 tau 단백질 중합체를 빠르게 형성하는 모델동물을 만들고 tau 단백질의 응집현상을 조절하는 유전자를 찾아내어 관련기작의 이해를 더욱 증진시키고자 하였다.

알츠하이머 환자의 뇌에서는 활성화된 caspase가 tau 단백질의 421번째 aspartic acid를 절단하는 일이 발생하며, 이에 생성된 절단된 형태의 tau 단백질(TauC3)은 *in vitro* 상태에서 빠르게 tau 단백질 중합체를 이룬다는 사실을 잘 알려져 있었으나 *in vivo* 상태에서 연구는 미진한 상태였다. 신경 특이적으로 TauC3 단백질을 발현하는 쥐 모델을 만들어 분석한 결과 1.3개월부터 빠른 기억력의 감소와 시냅스 밀도의 감소가 tau 단백질 중합체의

증가와 함께 나타나는 것을 볼 수 있었다. 또한 복강주사(*i.p.*) 또는 뇌강내 주사(i.c.v.)를 통한 메틸렌블루나 콩고레드와 같은 tau 중합 억제제 투여나 rapamycin과 같은 자가포식작용(autophagy) 촉진제 투여시 기억력의 향상이 tau 중합체 감소와 수반되어 나타나는 것을 관찰 할 수 있었다. 이를 통해 tau 단백질 중합체의 형성이 tau 관련 퇴행성 뇌질환과 비례적으로 나타나며 이 과정에서 TauC3 형태의 tau 단백질이 중요한 역할을 함을 알 수 있다.

또한 이 논문에서 우리는 tau 응집현상을 조절하는 새로운 유전자로 *POLDIP2*를 동정했다. POLDIP2는 치매 환자의 뇌가 노출된 유해한 환경을 대변하는 아밀로이드 베타(Aβ), TNF-α, 또는 과산화수소 등에 의해 양이 증가하였다. 또한 POLDIP2를 과발현 시킨 경우 tau의 인산화에는 크게 영향을 미치지 않으나 tau 응집현상은 크게 증가시키며 POLDIP2 발현을 감소시킨 경우 과산화수소 처리에 의한 POLDIP2 증가에 의해 나타나는 tau 단백질 응집현상의 증가가 나타나지 않는 것을 발견했다. 이러한 POLDIP2의 tau 단백질 응집현상 조절은 본 단백질의 DUF525 영역에 기반한 자가포식작용 (autophagy)과 일부 유비퀴틴에 의한 단백질 분해조절 시스템 (ubiquitin-proteasome system, UPS)의

조절을 통해 이루어진다. POLDIP2의 초파리 유사유전자인 CG12162의 돌연변이를 이용한 실험에서 Tau가 눈에서 과발현 된 초파리 모델에서 CG12162의 발현을 감소시키면 초파리의 눈의 망가짐이 완화되는 것을 확인하였고 Tau^{R406W}가 신경세포에서 과발현 되어 수명을 단축하는 초파리 모델에서 CG12162의 발현 감소가 수명을 증가시키는 것을 확인하였다. 이러한 관찰을 통해 POLDIP2가 tau 단백질 응집을 자가포식작용을 통해 조절하는 유전자로 동정하였으며, 이를 통해 tau 응집현상의 분자기작을 이해에 기여를 한다 할 수 있겠다.